Counter electrode materials based on carbon nanotubes for dye-sensitized solar cells

# Counter electrode materials based on carbon nanotubes for dye-sensitized solar cells

*Shahzad, N.[a], Lutfullah[b,c], Perveen, T.[b,d], Pugliese, D.[e], Haq, S.[f], Fatima, N.[g], Salman, S. M.[c], Tagliaferro, A.[e], Shahzad, M. I.[b,*]*

[a] US-Pakistan Centre for Advanced Studies in Energy (USPCAS-E), National University of Science and Technology (NUST), 44000-Islamabad, Pakistan.

[b] Nanosciences and Technology Department (NS&TD), National Centre for Physics (NCP), 44000-Islamabad, Pakistan

[c] Department of Chemistry, Islamia College Peshawar (ICP), University Campus, 25120-Peshawar, Pakistan.

[d] Department of Chemistry, Quaid-i-Azam University (QAU), 44000-Islamabad, Pakistan

[e] Department of Applied Science and Technology (DISAT), Politecnico di Torino, 10129-Turin, Italy.

[f] Chemistry Department, Azad Jammu & Kashmir University (AJKU), Muzaffarabad, Azad Kashmir, Pakistan

[g] Department of Chemistry, Bacha Khan University (BKUC), Charsadda, Pakistan.

***Corresponding Author: Shahzad, M. I. (PhD)**

Nanosciences and Technology Department (NS&TD), National Centre for Physics (NCP), Quaid-i-Azam University (QAU) Campus, Shahdra Valley Road, 44000-Islamabad, Pakistan. Email: imran.shahzad@ncp.edu.pk, imran-shahzad@live.com, Phone: +92 313 6961143

## Abstract

Efficiency, stability, and cost-effectiveness of are the prime challenges in research of materials for solar cells. Technologically as well as scientifically, attention gained by dye-sensitized solar cells (DSSCs) stems from their low material and fabrication costs and high efficiency projections. The objective of this study is to explore the the carbon nanotubes (CNTs) based counter electrode (CE) materials for DSSCs and to reconnoiter the suitable alternative materials in place of noble metals such as Pt, Au etc. Various classes of counter electrode materials based on CNTs including pure single walled, double walled, and multiwalled CNTs, doped CNTs and their hybrid composites with various polymers, metal and semiconducting oxides are discussed comprehensively in light of the research work started since the inspection of DSSCs and CNTs. The properties, associated with such materials including surface morphology, structural determination, thermal stability, and electrochemical activity, are also thoroughly analyzed and compared.

## Keywords

Carbon nanotubes; dye-sensitized solar cell; counter electrode; cyclic voltammetry; electrochemistry; photovoltaics.

## Highlights

- Comprehensive details about the DSSCs, their working principal and new materials for their various components are discussed.
- The role of carbon nanomaterials as counter electrode of DSSCs is discussed.
- Counter electrode materials based on CNTs are discussed and reviewed in details
- CEs based on pure CNTs, doped CNTs, CNTs-polymer, CNTs-hybrid, CNTs oxide/sulfide composites are reviewed in light of extensive literature survey since the inception of DSSCs and CNTs.

## Graphical abstracts

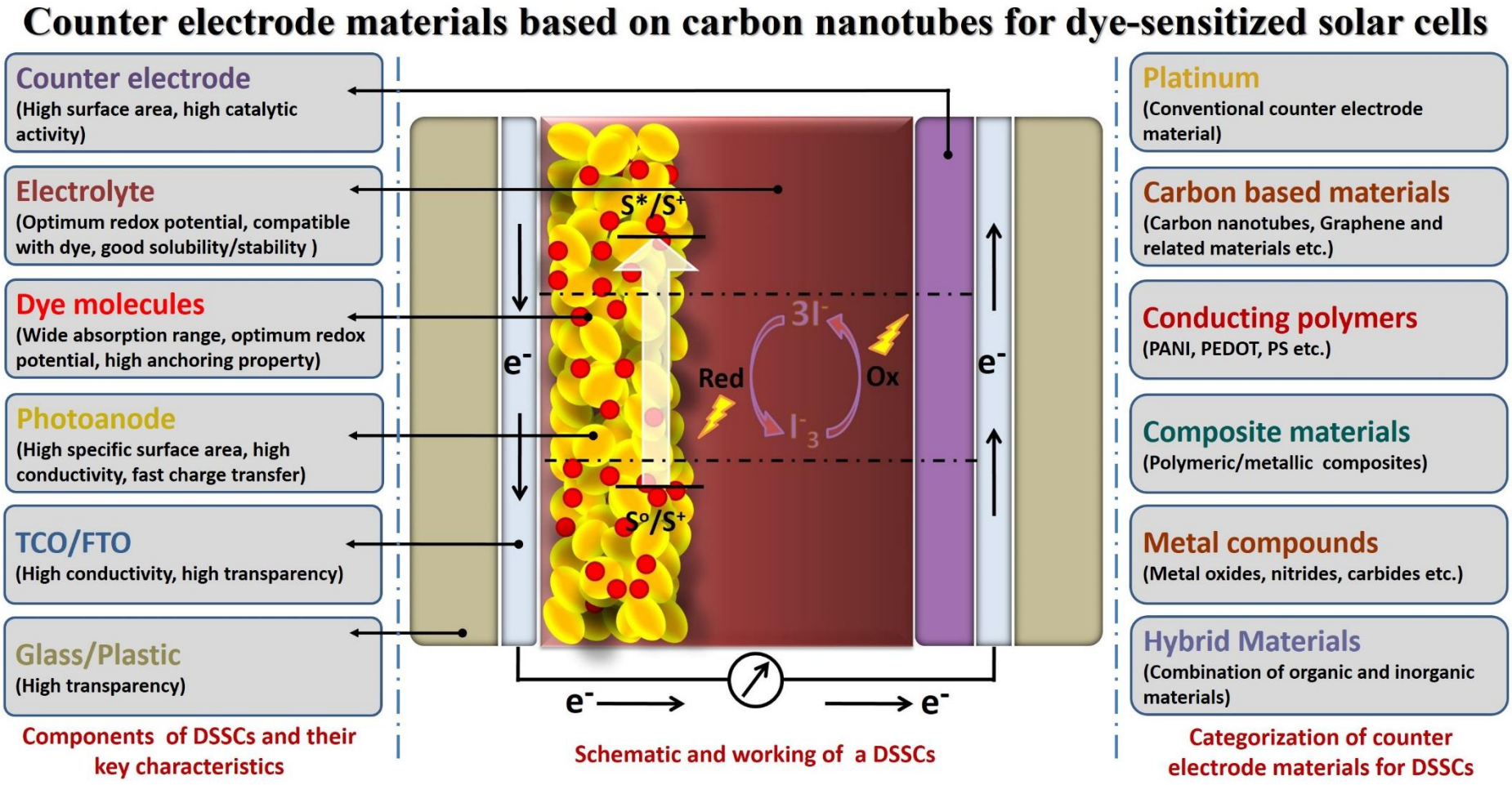

# 1 Introduction

The main challenge for humanity in the present scenario is the development of reliable, clean, and low-cost energy sources, since the world is passing through a phase of energy crisis due to the rapid increase in population and industrialization. Fossil fuels, which are the primary energy source, contribute to almost ~80% of the world total energy consumption. These are non-renewable energy sources destined to run out over time [1]. Furthermore, they also cause emission of carbon dioxide, which is the greenhouse gas most, responsible for global warming [2]. The remaining ~20% of the energy is provided by utilizing renewable and nuclear energy sources [1]. The renewable resources such as wind, hydro and solar power etc. are clean energy resources; therefore, it is need of hour to increase their share in total world energy market in order to address the problems associated with non-renewable energy sources and to keep the environment clean. Solar energy is the most appropriate source among all others because it exploits the abundant energy reserve of 174,000 TW that is annually provided to the earth by the sun [3]. Therefore, development of solar power will lessen the problem of energy crisis, limited reserves, and global warming.

Nanomaterials have great potential in developing solar power and increasing its shares because they possess peculiar properties which can provide breakthrough solutions to the problems hindering the progress of solar technology [4]. They also have enormous prospects in various other fields of life, including biotechnology [5], energy storage [6], medicine [7] and information technology [8]. Because of their dimensions in the nanometer scale, these materials exhibit high specific surface area. Furthermore, the nanomaterials in the form of tubes, particles, rods, and sheets possess unique physical, structural, chemical, electrical, and mechanical properties, which can bring benefit in diverse applications. Therefore, using nanomaterials as light harvester, catalyst, electron accumulator and electron transporter in solar cells will increase the overall efficiency of cells and ultimately rise world energy share [4].

Solar cells are devices that are used for conversion of sunlight into electricity through the photovoltaic effect. The share of solar energy in producing electricity was 1.9% toward the end of 2017 [1], which is 26% higher than that of 2016 [9]. It was further raised to 2.4% by the end of 2018 [10], thus showing that the adoption of solar energy technologies has experienced a constant growth in recent times as it is an economical and environmental friendly source of energy having wide reserves. In recent years, different types of photovoltaic devices have been studied which includes; a) silicon based first generation solar cells [11] showing power conversion efficiency (PCE) of 25% [3], b) second generation solar cells focused on thin films of different materials [12] exhibiting PCEs ranging between 20 and 28% [3], and c). emerging photovoltaic technologies commonly known as third generation solar cells [13] (see **Fig. 1**).

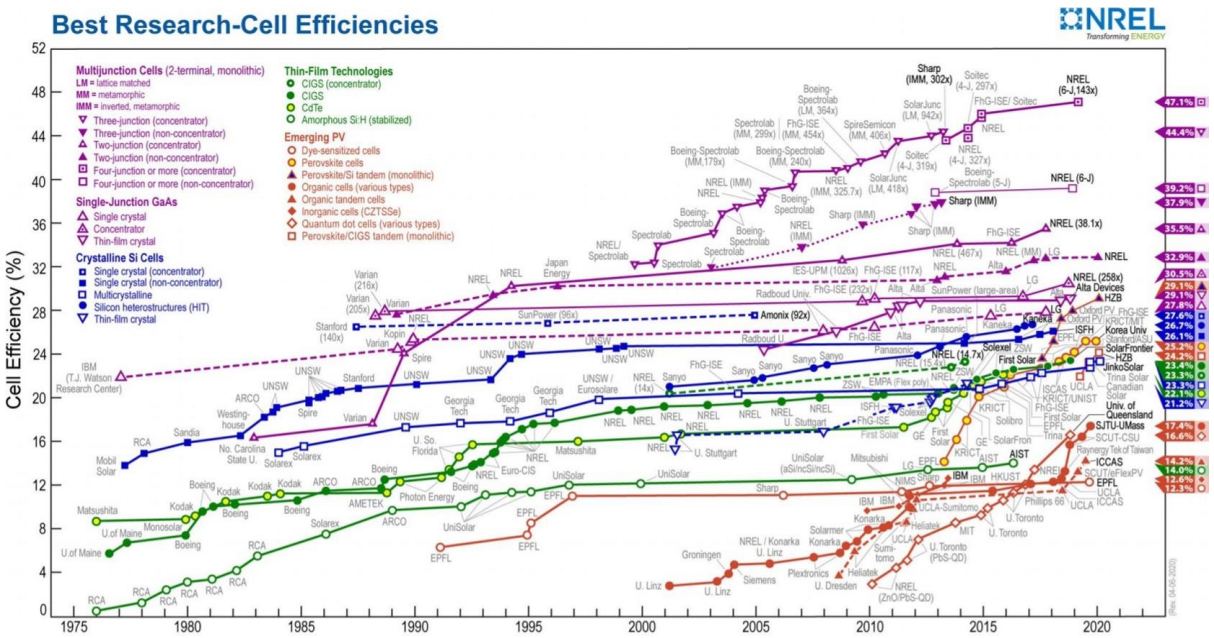


**Fig. 1. Best Research Cell Efficiencies [13] (The plot is courtesy of the National Renewable Energy Laboratory, Golden, CO.)**

First and second generation solar cells are able to provide the highest photo-conversion efficiency at present, but at the same time they are highly expensive due to their complicated fabrication process and high material cost. Within this framework, in order to get low cost energy harvesting devices with high efficiency and stability, emerging PV technologies have

been introduced. These emerging devices include dye-sensitized solar cells (DSSCs) [14] (PCE~14.3% [15], theoretically predicted 32% [16]), perovskite solar cells (PSCs) [17] (PCE~25.2% [13], theoretically predicted 30.5% [18]), organic/polymer solar cells [19] (PCE ~11.5%) and quantum dot solar cells [20] (PCE~13.43% [21], theoretically predicted more than 65% [4]). One of the key elements of these third-generation solar cells is the electrocatalyst layer. The role of electrocatalyst layer in energy harvesting devices is of paramount significance, as it supports electrons accumulation from the external circuit and catalyzes the process of electrolyte reduction [22].

DSSCs were firstly introduced by Grätzel in 1991 [23]. The electrocatalyst layer, which is commonly known as counter electrode (CE), contains a conductive glass, which enhances the rate of electron transfer and decreases the recombination. It is coated with a catalyst, usually platinum (Pt), which is considered as one of the best catalytic CE materials used in DSSCs. It shows good catalytic activity, electrical conductivity, stability and efficiency [24]. However, there are several drawbacks exhibited by Pt electrode. The abundance of Pt in the Earth's crust is very low, which inevitably leads to high cost and makes its large scale production difficult [25]. Furthermore, Pt has low corrosion resistance against Iodide/Triiodide, which is the most common redox couple employed in DSSCs electrolyte. Therefore, alternative classes of materials are being intensively investigated. Carbon based materials such as carbon nanotubes, carbon black, fullerene and graphene are the most common among them. Carbon nanomaterials display several forms, i.e. zero dimensional fullerenes [26], 1-dimensional carbon nanotubes (CNTs) [27] and 2-dimensional graphene [28]. Due to their exceptional chemical and physical features, these materials are applied in various fields, particularly in energy harvesting [29] (solar cells [30] and fuel cells [31]) and energy storage [32] (batteries [33] and supercapacitors [34]). Carbon nanotubes (CNTs) are well recognized for their combined advantages of elevated aspect ratio enhanced specific surface area and remarkable electrical and thermal

conductivities. Because of these properties, CNTs are good candidates as alternative electrocatalyst [30]. In recent years, these materials along with their composites with various metal oxides and polymers have been studied as CE materials [35].

In this review, the advantages exhibited by carbon nanotubes based CEs are comprehensively discussed. These electrodes have been employed several times as CEs in DSSCs, but they might have applications also in other sensitized solar cells and energy storage devices. Before broadly stating the progress towards replacing the precious Pt with low cost and easy to fabricate CNTs electrodes, we will briefly discuss the components and the working principle of DSSCs, focusing on the role of the CE in achieving a smooth and efficient functioning of these devices.

## 2 Components and Working Principle of DSSCs

DSSCs have great potential to replace silicon-based solar cells because of their low cost, flexibility, semi-transparency, durability, and simple assembling process. A typical DSSC contains a dye-loaded $TiO_2$ electrode deposited on a conductive glass substrate (usually FTO), $I^-/I_3^-$ based electrolyte solution and a Pt counter electrode (see **Fig. 2**).

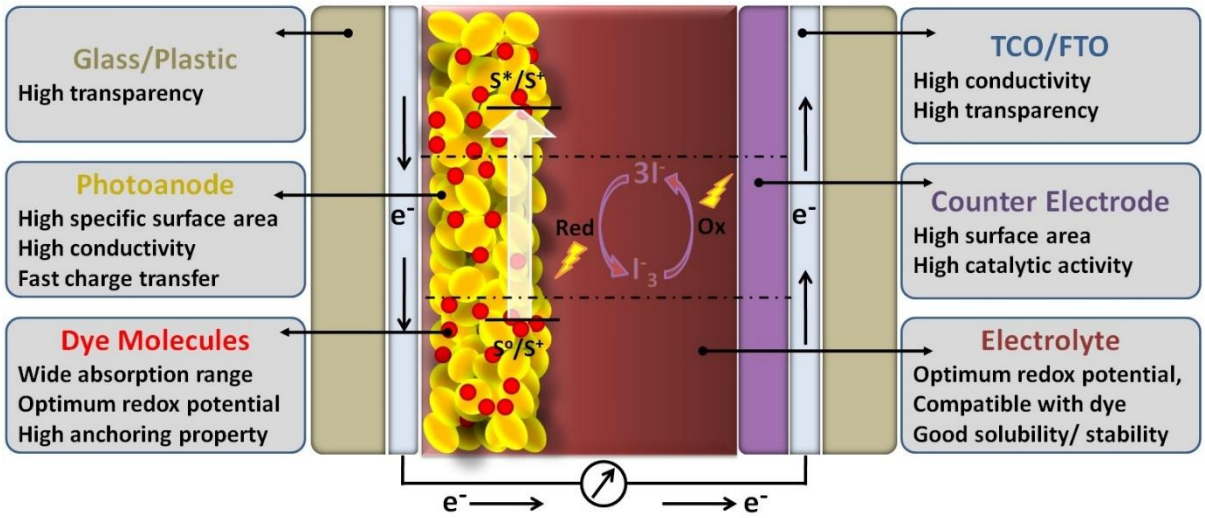


**Fig. 2. Working mechanism of a dye-sensitized solar cells (DSSCs)**

The dye molecules introduce electrons into conduction band of the $TiO_2$ layer upon illumination. The electrons are then diffused through the nanostructured film of $TiO_2$ and are accumulated at the front contact of FTO. A closed regenerative circuit is obtained by the redox couple ions present in the electrolyte, which drain the electrons from the external circuit at the counter electrode and reduce the oxidized dye molecules [36].

## 2.1 Sensitizer

The sensitizer, commonly known as dye, is the key component of a DSSC. The main function accomplished by the sensitizer is to absorb photons and to produce electrons, which are successively transferred into the conduction band (CB) of the semiconducting oxide. For its efficient performance, the sensitizer needs to reveal suitable lowest unoccupied molecular orbital (LUMO) and highest occupied molecular orbital (HOMO) in order to promote a higher charge injection in the CB of the semiconductor oxide followed by dye regeneration from the redox electrolyte, enhanced molar extinction coefficient in the visible and near-infrared regions and improved solubility and photostability [37]. It should also possess groups in its structure which help its chemisorption on the semiconductor oxide and should be able to sustain 108 redox turnovers, which correspond to an operation life time of 20 years [38, 39].

Numerous sensitizers are employed in DSSCs, like metal complex [40], metal-free organic [41], and natural dyes [42]. The most common sensitizer for DSSC is Ruthenium (II) polypyridyl [43], because of its various beneficial characteristics such as high absorption, extended excited-state lifetime and enhanced metal-to-ligand charge transport properties. The light absorbing capability of Ruthenium polypyridyl is extended approximately up to 350 nm [44]. The highest reported efficiencies achieved by the Ru (II) dye based DSSCs were 11.2% in 2005 [45] and 11.7-12.1% in 2010 [46].The relatively low molar extinction coefficient and the high cost are the main drawbacks showed by Ru (II) polypyridyl dyes [47]. Metal free organic dyes are an alternative class of materials that are being intensively investigated since

2004, and their employment has led to a noticeable solar cell efficiency of around 10% [48]. Co-sensitization of these dyes can further enhance the DSSC photovoltaic performance, and Yella et al. in 2011 achieved a maximum efficiency of 12.3% (which exceeds 13% under a different light intensity) by co-sensitizing zinc porphyrin dye with another organic dye [49]. The same 13% efficiency was also achieved by Mathew et al. in 2014 using a single dye without co-sensitization [50]. The efficiency was further enhanced up to15% by using co-sensitization of organosilicon based dyes [51]. A study on metal free dyes has reported an efficiency of 12% using a phenothiazine based metal free organic dye [52]. In the category of metal free sensitizers, the maximum efficiency of 12.6% has been achieved by employing a noncyclic aromatic hydrocarbon, N-annulated benzoindenopentaphene (NBIP) based metal free D-A dye C293 without using any co-adsorbent [53]. Natural dyes are reliable alternatives to expensive organic dyes thanks to their low cost, easy extraction and non-toxicity. The maximum efficiency achieved using these dyes are 2.06 and 2.00% for purple wild Sicilian prickly pear dye and pomegranate dye, respectively [54].

Other classes of sensitizers include inorganic semiconductor quantum dots (QDs) [55] and perovskite material based dyes. QDs based dyes exhibit certain significant characteristics such as changeable band gap energy, which strongly depends on the QDs size and shape, greater light absorption coefficients, high dipole moments and several extraction and generation features. All these properties make them suitable sensitizers for DSSCs with efficiency reaching 13% [56]. The maximum efficiency (13.43%) was achieved by using cesium based colloidal QDs [21]. Perovskite materials, displaying a band gap lower than 1.5 eV, were first investigated in 2009 as sensitizer in DSSCs showing a conversion efficiency of approximately 4% [57]. Further research on these materials showed promising results, i.e. an efficiency near 22.1% was achieved by using mixed halide based perovskite materials [58]. This efficiency was further increased to 23.3% and another study reported a maximum efficiency of 25.5% in

2019 [13]. Despite their noticeable photovoltaic performance in DSSCs, nevertheless perovskite materials suffer for important disadvantages: they are not environmental friendly, since they contain hazardous heavy metals, and they show phase transition at the solar cell operation temperature range, instability with variation in pressure and temperature and sensitivity to the moisture present in the environment [58].

## 2.2 Photoanode

A semiconductor film, usually termed as photoanode, plays a vital role in the operation of DSSCs. The key functions played by the photoanode are to support the sensitizer, accept the electrons from the sensitizer and to transport those photoexcited electrons to the external circuit. Therefore, ideally, a photoanode should possess vast surface area for dye loading and suitable band gap, which will enable it to effectively accept and transfer electrons to the external circuit. Usually the criteria demand the conduction band of semiconductor to be 0.2 or 0.3 eV lower than that of the sensitizer [59]. Apart from that, the band gap should be large enough to effectively transfer all the illuminating light to the sensitizer with minimum losses and the structure should possess least number of crystal boundaries and defects in order to lessen the recombination process of electrons [60].

DSSCs photoanodes are commonly constituted by a thick film (10 μm) of $TiO_2$ [61], as it displays the advantages of being cheap, abundant, nontoxic, biocompatible, and it also possesses an appropriate band structure [39]. $TiO_2$ in various morphologies such as 1D nanoparticles, nanotubes, nanowires, nanorods and 3D hierarchal structures such as spheres or beads has been employed as photoanode in DSSCs. By utilizing this morphology engineering strategy, an efficiency as high as 10% was reported by several researchers [60]. Other semiconductors have also been applied as photoanode in DSSCs because they possess similar band structure to that of $TiO_2$ and bring their own unique characteristics to the cell. These semiconductors include ZnO [62] (extensively studied after $TiO_2$), $SnO_2$ [63], $Nb_2O_5$ [64], $WO_3$

[65], $Ta_2O_5$ [66], CdSe [67], CdTe [68], CdS [67] and PbS [69] nanostructures. To improve the performance of the photoanode, these nanostructures can be doped with various ions such as $Zn^{2+}$, $La^{3+}$, $Nd^{3+}$, $Er^{3+}$ and $Ho^{3+}$ and can also be decorated with different noble metals such as silver, chromium, copper, and gold [70].

## 2.3 Electrolyte

The electrolyte in DSSCs performs the task of dye regeneration after the electron injection in the semiconducting photoanode conduction band and is responsible for the inner charge carrier transport between the two electrodes. Therefore, the most relevant electrolyte characteristics are: (i) large electrical conductivity; (ii) rapid distribution of the electrons due to little viscosity; (iii) high interfacial interaction with the nanostructured photoanode and the CE; (iv) low affinity for sensitizer desorption from the oxidized surface i.e. dye extraction; (v) reduced light absorption in the visible range [39]. The role of the electrolyte is vital as it affects both the stability and the efficiency of DSSCs. The electrolyte contains redox ions, which act as mediators between the photoanode and CE. The most commonly employed electrolyte is based on the iodide/triiodide redox couple dissolved into an organic matrix, which allowed achieving an efficiency of 11.7-12.1% [46]. Despite their promising photovoltaic performance, nevertheless the $I^-/I_3^-$ based electrolytes display some important drawbacks, such as leakage and contamination of the environment with organic components and volatilization of the redox couple, which lowers its concentration and leads to the increase of the cell's internal resistance [71]. Other redox couples have also been investigated, and recently Kakiage et al. achieved a maximum efficiency of 14.3% by employing a cobalt-based redox shuttle in combination with a Pt-free CE [51].

To overcome the problems related to the liquid electrolytes such as electrolyte sealing, volatility of solvents and long term stability [72], several strategies have been proposed such as replacing liquid electrolytes with quasi-solid [71] and solid [73] ones. Quasi solid-state

electrolytes are electrolytes possessing the stability of solids and the mobility of liquids. They are prepared by solidifying liquid electrolytes with the help of organic or inorganic gelators. The maximum efficiency reported for these electrolytes is higher than 10%, however, they still highlight the disadvantage of leakage because of liquid component [74]. To overcome the leakage issue, in recent years, solid state electrolytes based on poly(vinylidinefluoride), poly(ethylene oxide), and poly(vinyl acetate) etc. have been thoroughly investigated [75]. The maximum power conversion efficiency achieved with conventional solid-state electrolytes is around 8% except for all solid QDs or perovskite solar cells, in which efficiency values of 13.34% [21] and higher than 20% [58] have been reported, respectively.

## 2.4 Counter electrode

An electrode is an electronic conductor, which assists the smooth flow of electrons through an electrolyte or any other medium. Commonly, two electrodes known as cathode and anode constitute a cell. In the DSSCs system, $TiO_2$ coated over FTO glass substrate constitutes the photoanode, while Pt coated FTO acts as cathode, also known as counter electrode. It serves three important functions, i.e. it accumulates electrons provided by the outer circuit, it catalyzes the process of electrolyte reduction [22], and it acts as a mirror for the unabsorbed light in order to enhance the overall efficiency of the cell [76]. These functions demand the CE to possess specific properties such as high conductivity, high electrocatalytic activity, high reflectance, mechanical, chemical, and thermal stability, appropriate energy levels with respect to the ones of the redox couple, good adhesion to the substrate, high surface area, and optimum thickness. Different catalysts have been explored as CEs for DSSCs, but the most commonly used is Pt.

Enhanced exchange current density, high electrocatalytic activity, high transparency and noticeable power conversion efficiency make Pt electrode a standard choice as CE in DSSCs [39]. Despite these promising features, it also possesses some disadvantages, such as high cost, limited availability, and corrosive behavior towards the electrolyte. Thus, noticeable research

efforts have been devoted to develop highly stable and more efficient electrodes featured by a low cost and an easy fabrication process. For this purpose, various materials such as metals [77], alloys [78], inorganic metal compounds [79-85], conductive polymers [86], carbon-based materials [87] and composites [88] have been proposed as CE in DSSCs. Among the various available materials, carbon nanomaterials and their composites with polymers and transition metal oxides are potentially suitable to replace the Pt electrode because of their huge abundance, large-scale production, high conductivity, high catalytic activity, large surface area, high thermal stability, low cost, excellent corrosion resistance towards iodine, and high reactivity towards iodine redox couple [89-91]. Moreover, the current density obtained in presence of carbon-based CEs is higher with respect to that of Pt electrodes because of the larger availability of catalytic sites. In the coming sections, we will highlight the progress in the replacement of the conventional CE materials (Pt) for DSSCs with CNTs based CEs.

## 3 The role of carbon as CE material for DSSCs

Carbon based materials can generate, store and transport energy. That's why they can be employed as promising electrode materials in various electronic devices [92], such as fuel cells [93], solar cells [94], batteries [95], super capacitors [96], water electrolysis systems [97], transistors [98], photo catalysis [99, 100] and hydrogen storage devices [101, 102]. We already mentioned that carbon nanomaterials are highly striking to be used in place of Pt CEs in DSSCs, as they possess promising properties. Graphitic constituants like graphite, graphene [103], carbon nanotubes [104], activated carbon [105], carbon black [106], carbon powder [107], carbon nanofibers [108] and their composites, metal oxide carbon compounds and poly aromatic hydrocarbon have also been used in DSSC as they are able to provide sufficient electrical conductivity to the thin film carbon electrodes. The efficiency achieved with carbon-based materials is quite good, thus encouraging the researchers to work on them to replace Pt and other rare metals based electrodes in DSSCs. In 1996 Kay and Grätzel used for the first

time a carbonaceous material for the CE fabrication achieving a device efficiency of 6.7% [2], which is lower than that obtained with a conventional DSSC (up to 10%) but still encouraging. The CE was fabricated starting from an aqueous dispersion of graphite powder, nanocrystalline $TiO_2$ and carbon black through doctor blade technique. Since then, the efficiency and stability of various carbon-based materials for DSSCs CE have been tested.

## 4 Carbon nanotubes based CEs for DSSCs

Nowadays the stability, efficiency, and cost of solar cells are the main challenges in the field of photovoltaics. Scientifically and technologically, interest gained by DSSCs is due to their low fabrication and materials costs and high efficiency forecast. CEs play a vital role in achieving high conversion efficiencies in DSSCs. In recent decades, CNTs have been deeply studied as a sound alternative to the conventional Pt in view of obtaining a cheaper CE for DSSCs. CNTs are allotropes of carbon structurally composed of graphene sheets rolled into a cylindrical shape. Based on the number of graphene layers staked one up to the others, respectively one, two or multiple, CNTs are commonly labeled as single walled carbon nanotubes (SWCNTs), double walled carbon nanotubes (DWCNTs) and multi walled carbon nanotubes (MWCNTs). Furthermore, CNTs are being used in their pure form as well as in composites one (see **Fig. 3**).

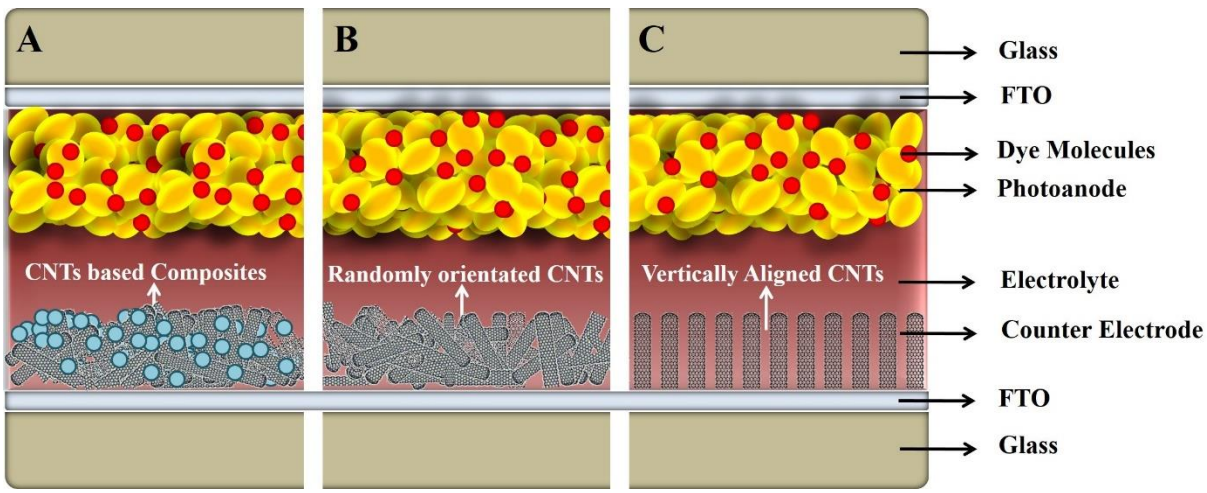

**Fig. 3. Different forms of CNTs used as CE materials of DSSCs.**

The nanometer scale and the unique geometric structure of CNTs make the electron transfer in a CNTs based film faster than in Pt based CE and thus its performance comparable to that of Pt. Efficiencies up to 13% were obtained with devices employing CNTs based electrodes [50].

### 4.1 Pure and modified CNTs based CEs

Pure CNTs of various types (i.e. SWCNTs, DWCNTs, and MWCNTs etc.), in different configurations (i.e. bundles, forest, vertically or horizontally aligned etc.), and with different modifications and functionalization have been studied as CE in DSSCs with promising performance. Owing to their high surface area and reduced sheet resistance, first time in history SWCNTs were successfully employed as CE material in DSSCs as a result of Suzuki et al. [109] efforts and consequently their performance was analyzed and compared with that of other electrodes. SWCNTs based CE films were prepared by ultrasonically mixing CNTs in water then dropwise placing the obtained suspension on FTO glass or filtering it through a Teflon membrane filter. The efficiencies achieved with such CEs were 3.5 and 4.5%, respectively. The higher efficiency in the latter case was attributed to the high conductivity and low charge transfer resistance of the membrane.

DWCNTs were also employed as CE for DSSCs because recently great improvements have been achieved in their manufacturing and refinement processes. They exhibit a double walled structure, which is intermediate between SWCNTs and MWCNTs, therefore they are expected to possess a greater thermal and chemical stability than those shown by the SWCNTs [110]. Zhang et al. fabricated a DWCNTs based CE by blending terpineol and ethyl cellulose and depositing the blend on a conducting FTO substrate via screen printing technique, followed by annealing at 300 °C [111]. The attained efficiency (~6.05%), catalytic activity and performance results were comparable with those of Pt based CEs (showing efficiency~6.80%). The

efficiency of DWCNTs based CEs was also investigated by Siuzdak et al. using a ruthenium-based dye. They achieved a maximum efficiency of 4.56%, which revealed to be greater than the 3.96% obtained with Pt. They made use of a cost effective spray coating technique for the preparation of the CE followed by annealing at different temperatures, out of which 300 °C annealed film produced the best results [112].

To boost the efficiency of DSSCs, MWCNTs were also employed for the fabrication of CEs. Lee et al. fabricated MWCNTs based CE on FTO glass and achieved an efficiency of 7.67% (Pt = 7.83%), which increased up to 7.96% (Pt = 8.03%) when light intensity was decreased down to 54 mW/cm$^2$ [104] (see **Fig. 4**). The electrode was prepared from a paste containing MWCNTs, organic binder and distilled water, along with carboxyl methylcellulose and sodium salt. Beside the good efficiency, these MWCNTs based CEs are very stable and show a lower charge transport resistance.

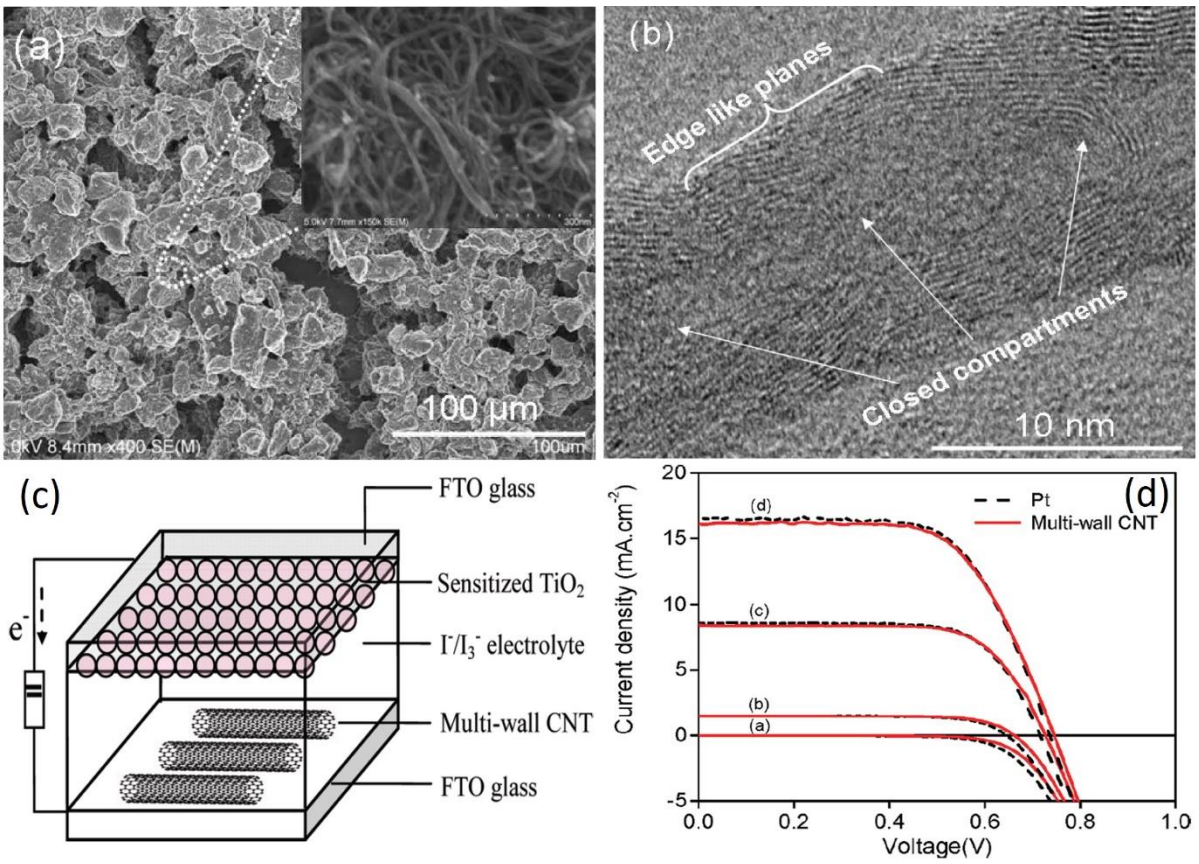

**Fig. 4. a). FE-SEM image of a MWCNTs composite film (Inset: enlarged view of the marked portion), b). TEM image of the bamboo-like structure in MWCNTs, c). Schematic of a MWCNTs CE based DSSC, d). Current-voltage characteristics of DSSCs with MWCNTs (solid line) and platinum (dashed line) counter electrodes. Curve (a) shows the performance of devices in the dark. Curves (b), (c), and (d) were measured under 0.1, 0.5, and 1 sun illumination (air mass 1.5 G), respectively. (Reproduced with the permission from Ref. [104], Copyright 2009 ACS Publications).**

Chen et al. studied the fabrication of CNTs based CEs by screen printing technique followed by calcination utilizing an ultrafast technique which made use of a nitrogen atmospheric-pressure plasma jet (APPJ) instead of a conventional calcination [113]. This method proved to be ecofriendly and cost-saving as the energy consumption per unit processing area was estimated to be 500 J/cm$^2$, which is approximately 1/5 than that spent for the synthesis of CEs via the traditional furnace technique. A maximum conversion efficiency of 5.65% was achieved at APPJ treatment time interval of 5 seconds, while an additional increase in the APPJ treatment time resulted in a decrease of the photovoltaic performance. Electrode thickness is an important parameter to be considered, since it affects the charge transfer resistance and conductivity of the film obtained. Ramasamy et al. [114] prepared a MWCNTs based CE on FTO conductive glass through spray coating technique, and a maximum efficiency of 7.59% was attained when the spraying time was increased to 200 (see **Fig. 5**).

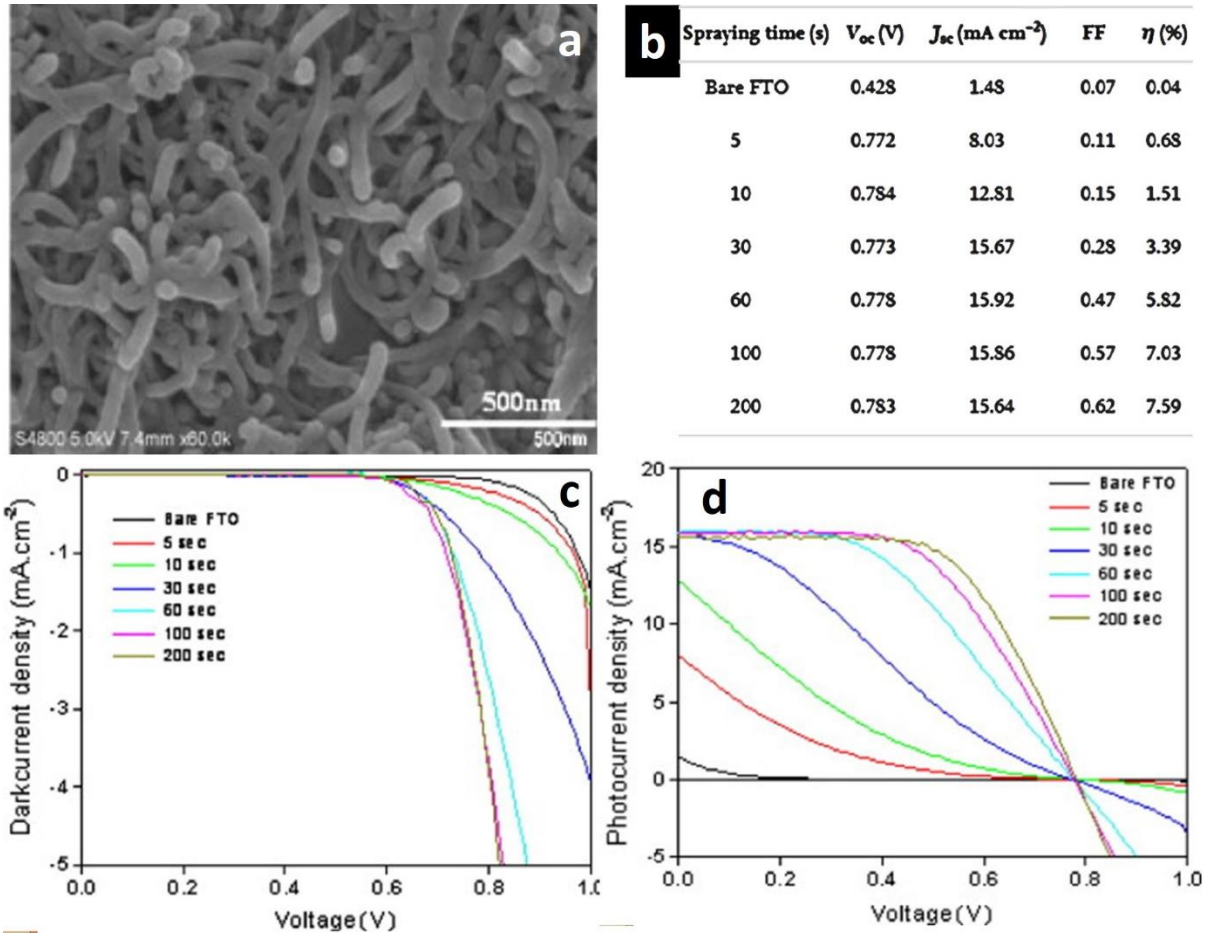


**Fig. 5. FESEM image of spray coated MWCNTs film on FTO substrate (a), performance comparison with respect to various spraying times (b), dark current density voltage (c) and photocurrent density voltage (d) of the DSSCs. (Reproduced wth the permission from Ref. [114], Copyright 2008 Elsevier).**

This was attributed to the decrease in MWCNTs charge transfer resistance while increasing the spraying time. Ahn et al. [115] prepared transparent and conductive MWCNTs based CEs on FTO glass by aerosol deposition process, achieving a maximum efficiency value of 5.18% when the deposition was carried out for 60 h and the thickness of the film obtained was equal to 42.5 μm. The efficiency was slightly higher than the one shown by the Pt based electrode (4.96%). By increasing the deposition time and consequently the thickness of the film, the overall conversion efficiency and current density of the CEs enhanced because of the low charge transfer resistance as well as improved catalytic activity.

CNTs are able to keep various structures like bundle, forest, vertical and horizontal alignments and random network [116-118]. These structures display a noticeable effect on the performance of the final device. In 2010 Nam et al. [119] used vertically aligned and randomly oriented MWCNTs, synthesized by the chemical vapor deposition (CVD) and screen printing techniques, respectively, as CE materials for DSSCs. A maximum photo-conversion efficiency of 10.04% was obtained by using the aligned CNTs based CE, while the devices employing the reference Pt and the randomly oriented MWCNTs based CEs showed lower efficiency values equal to 8.80 and 8.03%, respectively. The higher efficiency exhibited by the aligned CNTs based CE was because of the higher surface area of the electrode. Seo et al. synthesized highly disordered MWCNTs using a low temperature thermal CVD process and successfully employed them as a CE material for DSSCs [120]. The CNT catalysts were effective in improving the fill factor (FF) value in DSSCs when used in combination with electrolytes with large molecules. In particular, the efficiency increased from 6.51 up to 7.13% by interchanging the traditional Pt catalyst with MWCNTs catalyst and $Li^+$ electrolyte with 1-butyl-3-methylimidazolium cations based electrolyte.

Several kinds of CNTs including SWCNTs, DWCNTs and MWCNTs have been employed by Zhang et al. as CEs for DSSCs for comparison purpose [121]. The electrodes were fabricated by screen printing technique using pastes constituted by the different CNTs and an organic binder. The conversion efficiencies obtained were 8.0, 7.61 and 7.06% for DWCNTs, SWCNTs and MWCNTs, respectively (see **Fig. 6**). Owing to their high specific area and chemical strength, the DWCNTs facilitate the electron transport rate among the CE and the electrolyte. However, the more complicated growth process of DWCNTs with respect to the ones of SWCNTs and MWCNTs represents a significant drawback of such CE [35].

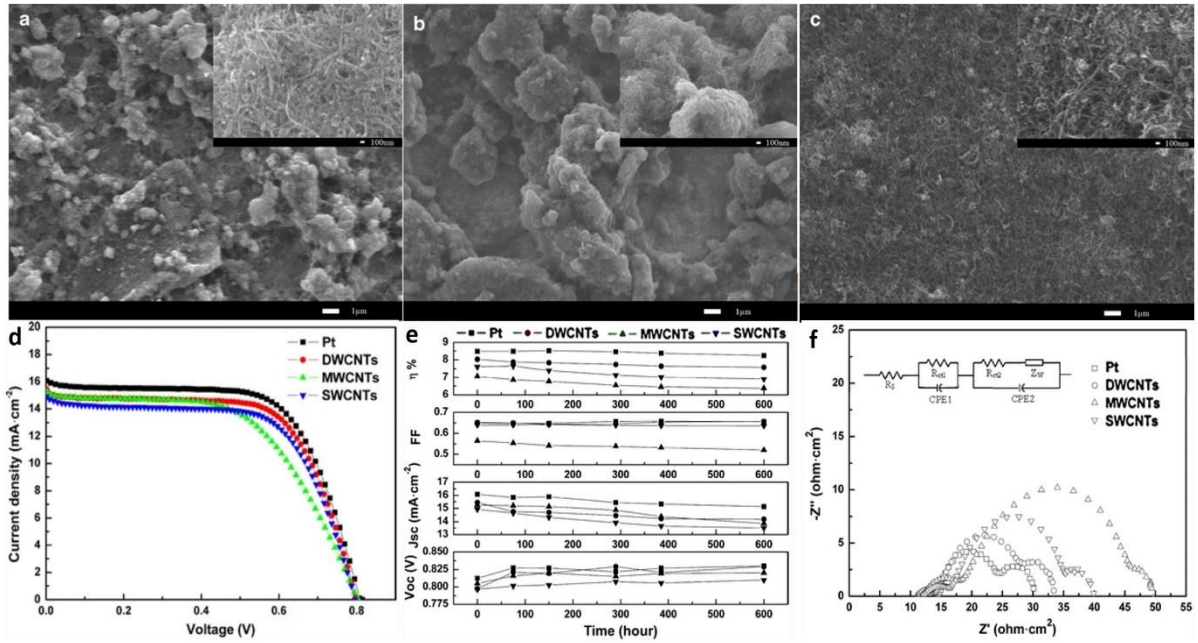


**Fig. 6. FESEM images of DWCNTs (a), SWCNTs (b), and MWCNTs (c) CE layers deposited on FTO substrates. Corresponding DSSCs photocurrent density-voltage (J-V) characteristics (d), short term evaluation of photovoltaic parameter (e) and Nyquist plots (f). (Reproduced wth the permission from Ref. [121], Copyright 2011 Springer).**

Despite nanocrystalline, $TiO_2$ revealed to be the most employed and efficient photoelectrode material in DSSCs, nevertheless it suffers from low inherent electron mobility. Consequently, materials with better conductivity have been commonly incorporated into $TiO_2$ or the latter has been replaced with other semiconducting materials displaying a greater mobility, such as ZnO and $SnO_2$. Recently, MWCNTs have also been investigated as CE material for DSSCs based on such alternative photoanodes. Younas et al. successfully employed MWCNTs as CE for $nWO_3$-$SnO_2$ photoanode based DSSCs [122]. A maximum efficiency of 6.12%, which was better than that showed by Pt CE (5.18%), was achieved when keeping to 1% the concentration of $nWO_3$ in the $TiO_2$ matrix. Similarly, Siwach et al. used MWCNTs for ZnO-graphene based DSSCs, and an efficiency of 2.04%, which is slightly lower than 3.17% of Pt CE based DSSCs, was obtained [123].

Noticeable research have been done nowadays to substitute the liquid electrolyte solid or quasi-solid electrolytes because the former suffers from the disadvantage of leakage, which ultimately affects the life time of DSSCs. MWCNTs were applied as CEs for those DSSCs as well. Arbab et al. [124] fabricated a quasi-solid state dye sensitized solar cell in which the electrolyte was made up of 5 wt% polyethylene (PEO) gel infused Poly(vinylidene fluoride-co-hexafluoropropylene (PVDF-HPF) with iodine based redox couple and the photoanode was based on $TiO_2$. The counter electrode, instead, was constituted by an ink made by functionalizing MWCNTs with cationic lipase enzyme followed by mixing with CMC and aging overnight. The uniform black ink was then spin coated over a chopped carbon fiber (CFF). The fabricated cell delivered an efficiency of 8.90%, which was slightly lower than that showed by a Pt/CFF based DSSC (9.78%). Similarly, Sun et al. [125] evaluated the compatibility of a CE based on lipase functionalized MWCNTs coated over FTO with liquid filled, gel filled and pristine electro-spun PVDF-HFP membranes. The efficiencies obtained for the different electrolytes containing DSSCs were 6.66% (liquid), 5.77% (gel) and 6.04% (membrane), which were analogous to the one obtained with Pt based CE. Chew et al. [126] also prepared gel polymer electrolyte based DSSCs and tested their efficiencies using as CE MWCNTs mixed with polyvinylpyrrolidone-co-vinyl acetate and coated on FTO using two techniques, i.e. spin coating and dropping methods . The electrolyte consisted of sodium iodide salt, polyacrylonitrile polymer, and 1-Hexyl-3-methyl-imidazolium iodide ionic liquid. The obtained efficiencies were 7.07 and 4.25% for spin coating and dropping methods, respectively, which revealed to be higher than/near the one achieved with Pt based CE (5.75%).

Functionalization of CNTs is commonly adopted to improve their dispersibility, adhesion to the substrate and to achieve a smooth and uniform film, which ultimately lead to the improvement of the performance for the targeted application. CNTs can be functionalized both covalently and non-covalently [127]. Different functional groups have been attached to CNTs,

such as acetonitrile, carboxylic acid and acetyl acetone [128]. Chou et al. prepared a CE film from SWCNTs functionalized with Tetraoctylammonium bromide (TAOB) dispersed in 2 different solvents, namely acetyl acetone and N,N-dimethylacetamide [129]. The as-prepared dispersions were coated onto FTO-covered glasses by drop casting technique and subsequently sintered at different temperatures. A maximum efficiency of around 1.2266% (Pt = 1.25%), ascribable to the better dispersibility of the SWCNTs, was achieved by employing the acetyl acetone dispersed SWCNTs based CE. To further enhance the performance of the CE, a silver (Ag) film was also placed between the FTO glass and the SWCNTs based electrode, thus leading to a drastic increase of the cell efficiency up to 1.3037%. Arbab et al. fabricated CEs for DSSCs composed of MWCNTs functionalized with different enzymes (laccase, glucose oxidase and lipase) [130]. The paste of the enzymatic solution of lipase was prepared in ethanol, followed by the addition of MWCNTs and carboxy methylcellulose (CMC) in the solution and aging overnight. The CE film was synthesized on FTO glass through tape casting method. The enzymatic functionalization of the MWCNTs allowed increasing the contact points between the CE and the electrolyte and enhancing the electron transportation, thus leading to a noticeable conversion efficiency of 7.52%.

The CNTs based CEs for DSSCs are commonly fabricated either by CVD method or by coating on FTO starting from a dispersion. Both these methods highlight some disadvantages, such as high cost, low scalability for the former while the latter suffers from pre-functionalization, which is essential to prepare a proper dispersion. To address these issues, recently Bernal et al. has recently employed few layer highly porous and well crystalline interconnected CNT fibers (CNTf), also known as CNTs yarns, both as CE and current collector in DSSCs [131] (see **Fig. 7c**). A remarkable photoconversion efficiency of 8.8% was obtained, which was higher than the 8.7% achieved with Pt based CE. Previously, Chen et al. applied aligned carbon nanotubes (ACNTs) fibers as both photo-electrode and CE of DSSCs achieving an efficiency of 2.94%,

which was comparable to that of Pt (3.3%) [132] (see **Fig. 7a**). Similarly, Pan et al. [133] has used ACNTs fibers both as photoanode and counter electrode of a DSSC and achieved efficiencies of around 7.33 and 5.97% employing organic thiolate/disulfide and iodine redox couples, respectively (see **Fig. 7b**). The efficiencies were remarkably higher than that obtained with a Pt based CE (2.06%).

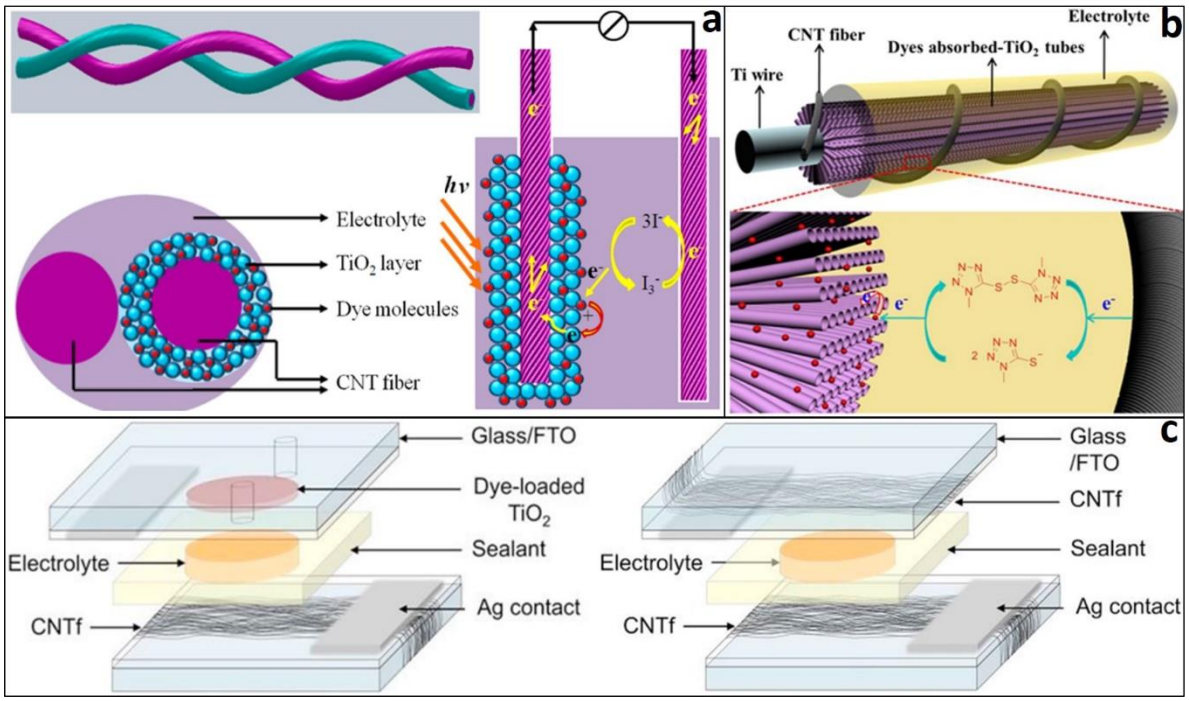


**Fig. 7. Schematic illustration of various configurations; a). Wire-shaped DSSC fabricated from two CNT fibers. (Reproduced with the permission from Ref. [132], Copyright 2012 ACS Publication), b). Photovoltaic wire with a CNT fiber as the counter electrode. (Reproduced with permission from Ref. [133], Copyright 2013 ACS Publication), and c) Typical and symmetric cells with CNTf based CE (Reproduced with the permission from Ref. [131], Copyright 2019 Elsevier).**

Z. Wei et al. [134] fabricated and compared different CE materials for DSSCs using untreated MWCNTs, acid-oxidized MWCNTs, graphite and platinum. They were able to achieve an efficiency of 3.1% with the CE containing nanographite, and acid-oxidized MWCNTs, which are higher than those, are obtained with all the other CE materials except Pt. The MWCNTs,

having diameters and lengths in the 10-20 and 100-500 nm ranges, respectively, were oxidized by an acidic mixture of $H_2SO_4$ and $HNO_3$. Due to the oxidation of MWCNTs, the photovoltaic performance of DSSCs showed an improvement as the resistance of the electrode based on treated CNTs was lower than that of untreated MWCNTs CEs.

Summarizes of the main characteristics and the photovoltaic performance of DSSCs assembled with pure CNTs-based CEs are tabulated in **Tab. 1**.

**Tab. 1. Main features and photovoltaic performance of DSSCs fabricated with pure CNTs based CEs**

| No. | CE Material | Deposition method | Photoanode | Sensitizer | Redox couple | PCE (%) | PCE vs Pt (%) | Ref. |
|---|---|---|---|---|---|---|---|---|
| 1 | MWCNTs | Doctor blading | $TiO_2$ | N719 | $I_3^-/I^-$ | 7.67 | 7.83 | [104] |
| 2 | SWCNTs | Filtration through membrane | $TiO_2$ | N719 | $I_3^-/I^-$ | 4.5 | 5.4 | [109] |
| 3 | DWCNTs | Screen printing | $TiO_2$ | D102 | $I_3^-/I^-$ | 6.05 | 6.80 | [111] |
| 4 | DWCNTs | Spray coating | $TiO_2$ | N3 | $I_3^-/I^-$ | 4.59 | 3.96 | [112] |
| 5 | MWCNTs | Screen printing<br>+ AJJP calcination | $TiO_2$ | N719 | $I_3^-/I^-$ | 5.65 | n.a. | [113] |
| 6 | MWCNTs | Spray coating | $TiO_2$ | N719 | $I_3^-/I^-$ | 7.59 | n.a. | [114] |
| 7 | MWCNTs | Aerosol deposition | $TiO_2$ | N719 | $I_3^-/I^-$ | 5.18 | 4.96 | [115] |
| 8 | VA-MWCNTs<br>RO-MWCNTs | CVD<br>Screen printing | $TiO_2$ | N719 | $I_3^-/I^-$ | 10.04<br>8.03 | 8.80 | [119] |
| 9 | Disordered MWCNTs | Low temperature CVD | $TiO_2$ | N719 | $I_3^-/I^-$ | 7.13 | 6.52 | [120] |
| 10 | f-SWCNTs<br>Ag Paste+f-SWCNTs | Drop casting | $TiO_2$ | N719 | $I_3^-/I^-$ | 1.2266<br>1.3037 | 1.25 | [129] |

| | | | | | | | | |
|---|---|---|---|---|---|---|---|---|
| 11 | SWCNTs<br>DWCNTs<br>MWCNTs | Screen printing | $TiO_2$ | N719 | $I_3^-/I^-$ | 7.61<br>8.03<br>7.06 | 8.49 | [121] |
| 12 | MWCNTs | Doctor blading | ZnO-GO | D749 | $I_3^-/I^-$ | 2.04 | 3.17 | [123] |
| 13 | Cationic f-MWCNTs | Spin coating | $TiO_2$ | N719 | $I_3^-/I^-$ | 8.90 | 9.78 | [124] |
| 14 | Lipase f-MWCNTs | Doctor blading | $TiO_2$ | D719 | $I_3^-/I^-$ | 6.66 | 7.32 | [125] |
| 15 | MWCNTs | Spin coating<br>Dropping method | $TiO_2$ | N719 | $I_3^-/I^-$ | 4.25<br>7.07 | 5.75 | [126] |
| 16 | Mesoporous CNTs fibers | n.a. | $TiO_2$ | N719 | $I_3^-/I^-$ | 8.8 | 8.7 | [131] |
| 17 | ACNTs fiber | n.a. | CNT-$TiO_2$ | N719 | $I_3^-/I^-$ | 2.94 | 3.3 | [132] |
| 18 | ACNTs fiber | n.a. | $TiO_2$ | N719 | $I_3^-/I^-$<br>thiolate | 5.97<br>7.33 | 2.06 | [133] |
| 19 | E-MWCNTs | Doctor blade | $TiO_2$ | D719 | $I_3^-/I^-$ | 7.52 | 8.00 | [130] |
| 20 | MWCNTs | Doctor blading | n$WO_3$-$TiO_2$ | N719 | $I_3^-/I^-$ | 6.12 | 5.18 | [122] |

## 4.2 Polymer coated CNTs and Polymer Composites based CEs

CNTs-polymer composite materials represent one of the most promising candidates for DSSC CEs due to their collective benefits including high specific surface area, brilliant electrical conductivity, noticeable electrocatalytic properties, high durability, good flexibility, rich supply, strong adhesion, and easy manufacture typical of polymers. For this purpose, several conducting polymers, such as Polyaniline (PANI) [135], Poly(3,4-ethylenedioxxythiophene) (PEDOT) [136], Polyvinylpyrrolidone (PVP) [137] and Polyvinylidene fluoride (PVDF) [138] have been used. Various processes have been tested for the CNTs-polymer composites synthesis. Electrodes conductivity is strictly affected by the CNTs amount and the thickness of the polymer layer. When the thickness of the polymer layer decreases, the porosity of the film increases, which leads to a better penetration of the electrolyte and reduced diffusion resistance. Polymer can serve various functions in preparing CEs. It can be used as conductive agent, dispersant and both carbon source plus dispersant to intensify the properties of MWCNTs as well as SWCNTs, which can act either as matrix or filler.

Hi et al. prepared covalently bonded SWCNTs/Polypyrole (PPy) composites by mixing pyrrole with SWCNTs through refluxing followed by in-situ polymerization [139]. Different concentrations of SWCNTs were added and a maximum efficiency of 8.30% was obtained with a concentration as high as 2.0 wt%. The better performance with respect to the one showed by bare PPy (6.31%) was attributed to the lower charge transfer resistance as the covalent bonding is established between the filler and the matrix.

Park et al. used polyvinylpyrrolidone (PVP) as dispersant and carbon source for synthesizing SWCNTs based CEs (see **Fig. 8**). They used simple casting technique for obtaining the film followed by calcination in order to remove binder and convert PVP (1wt%) which was wrapped smoothly around SWCNTs into carbon. The PVP presence resulted in a smooth and uniform film without aggregation of CNTs. The film was subsequently employed as CE of a DSSC and

showed a photoconversion efficiency of 4.5%, which was higher than that exhibited by the bare SWCNTs film (2.34%). The improved photovoltaic performance is mainly because of the lower charge transfer resistance induced by the presence of PVP [137].

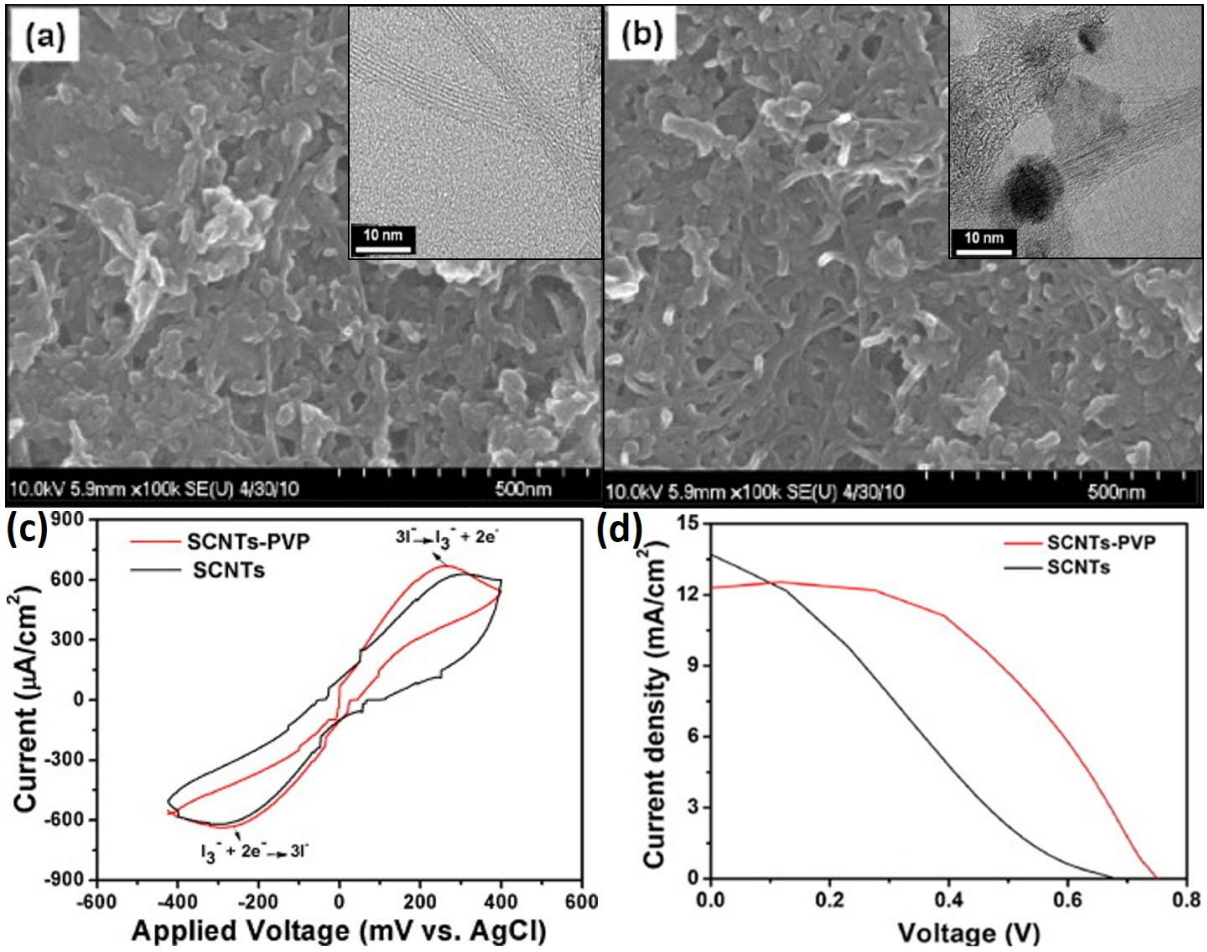


**Fig. 8. SEM and TEM (inset) images of SWCNTs based electrodes without (a) and with (b) PVP, cyclic voltammetry in acetonitrile (c), and J–V curve of DSSCs under light intensity of 100 mW/cm$^2$ (d). (Reproduced with the permission from Ref. [137], Copyright 2012 Elsevier)**

MWCNTs were also applied as filler or matrix with PEDOT polymer for preparing CEs. Lee et al. prepared PEDOT and PEDOT/MWCNTs based CEs for application in DSSCs [140]. The efficiency achieved with PEDOT was 7.44% when PEDOT/imidazole was kept equal to 2.0. The efficiency was slightly lower than that exhibited by Pt-sputtered electrode (7.77%) which

may be attributed to the increase in the reaction rate of the redox couple regeneration because of the large specific surface area. They further incorporated MWCNTs into PEDOT and spin coated them on different substrates at different spin rates. The highest efficiency of 8.08% was achieved with stainless steel substrate at a spin rate of 370 rpm and MWCNTs concentration of 0.6%. Shin et al. developed CNT/PEDOT composite based CE for DSSCs by chemical oxidative polymerization using iron chloride ($FeCl_3$) and dodecyl benzene sulfonic acid (DBSA) as oxidant and surfactant, respectively [141] (see **Fig. 9**) . PVDF was employed as a binder and the viscous paste obtained was directly painted over FTO for CE fabrication. An enhanced efficiency of about 4.62% was achieved, in comparison to those obtained with pure CNT CE (3.88%) and PEDOT CE (4.32%).

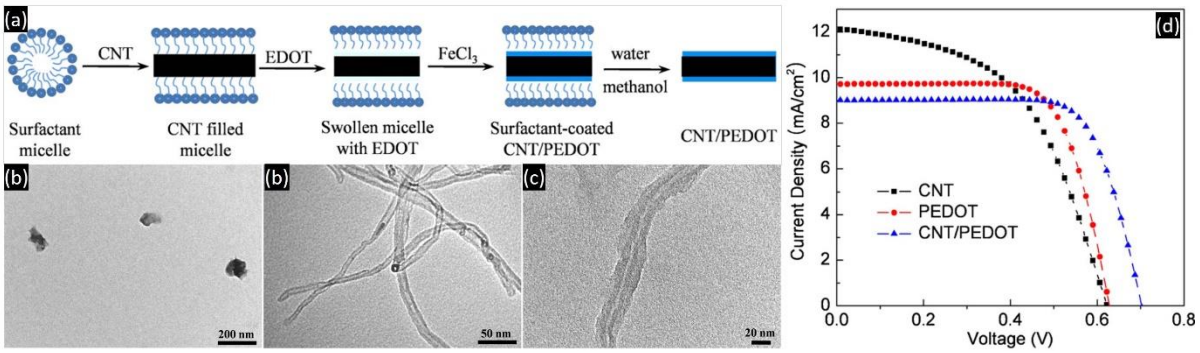


**Fig. 9 Schematic illustration for the synthesis of CNT/PEDOT core/shell nanostructures (a). SEM images of PEDOT (b), CNTs (c), and the CNT/PEDOT (d) nanostructures. J–V curves of DSSCs using various counter electrode materials (e). Reproduced with the permission from Ref. [141], Copy right 2011 Elsevier)**

PEDOT:PSS can be used to improve the dispersion of MWCNTs in the solvent as well as their electronic conductivity. Fan et al. fabricated CEs by using MWCNTs dispersion prepared with the help of PEDOT:PSS or polystyrenesulfonate acid (PSSA) as dispersing agent [142]. The solution was coated over FTO utilizing spin coating technique and the DSSC efficiency obtained with the two different dispersants were 6.5 and 3.6%, respectively. The difference

between the efficiency of the two dispersants containing composites is linked with the different nature of the interactions involved. The π-π interactions present in the PEDOT:PSS containing composite are responsible for the increase in the electron transport, while PSSA containing composite is featured by hydrophobic interactions which lead to an insulating barrier for electron transport, as PSSA itself is non-conducting. The efficiencies were lower than that showed by the Pt based CE (8.5%) but still promising. Recently, Yun et al. [143] prepared PEDOT:PSS dispersed MWCNTs based CEs by spin coating technique and achieved an efficiency as high as 6.1% . They used MWCNTs with various purities and diameters and carried out an acid treatment. The highest efficiency was achieved for MWCNTs with >85% purity, diameter in the range 8-15 nm and subjected to acid treatment.

Recently, Ma et al. [144] also utilized PEDOT:PSS as well as Triton-X100 and a blend of the two polymeric materials for aligned MWCNTs functionalization. The best efficiency of 3.85% was achieved for PEDOT:PSS modified aligned MWCNTs due to the low charge transfer resistance. Other complex polymers are also used for functionalization of MWCNTs. Choi et al. used pyrene functionalized block copolymer poly(maleic acid-co-phydroxystyrene)-block-poly(p-hydroxystyrene) (HSPM) for functionalization of MWCNTs and obtained an efficiency of 5.94%, which was slightly higher than that achieved with a bare CNTs (10 wt%) based CE fabricated by screen printing technique (5.69%) [145].

Recently, Li et al. prepared a honeycomb PEDOT/MWCNTs based CE by using spin coating technique for MWCNTs and PMMA deposition followed by electrodeposition of PEDOT [146](see **Fig. 10**). The dissolution of PMMA in chloroform gave rise to the honeycomb morphology. The as-prepared film was employed as CE in bifacial DSSCs. High efficiencies equal to 9.07 and 5.62% were achieved for front and rare illumination, respectively, in comparison to 7.51 and 3.49% obtained in presence of the bare PEDOT CE.

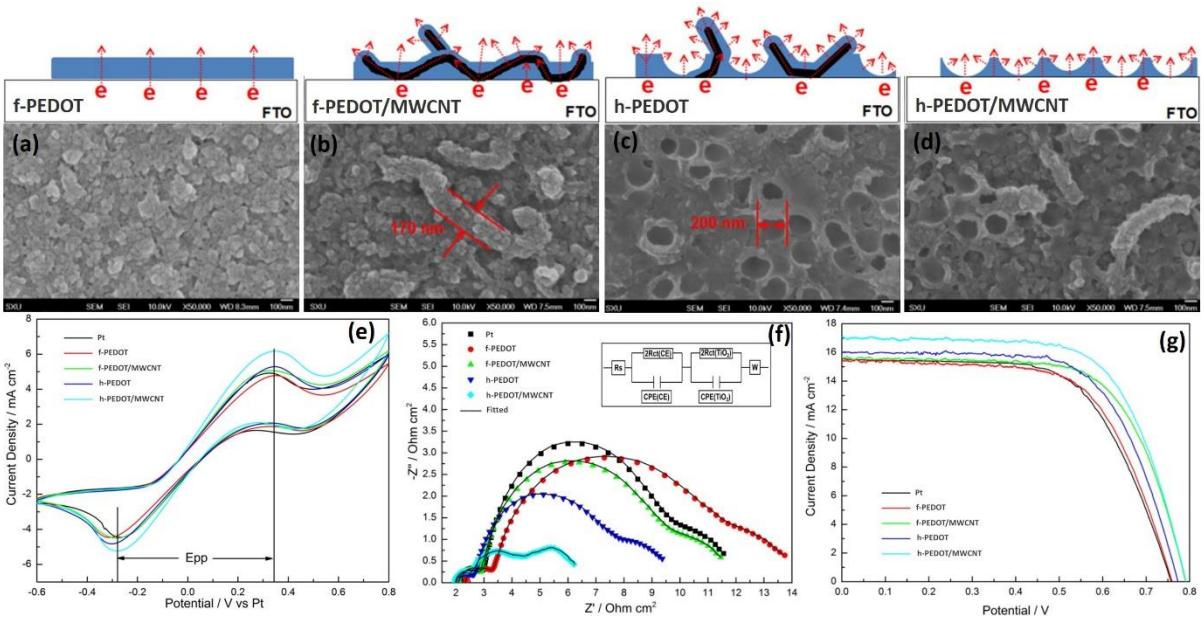


**Fig. 10. SEM images and electron transport paths in f-PEDOT (a), f-PEDOT/MWCNT (b), h-PEDOT (c) and h-PEDOT/MWCNT (d) based CEs. Cyclic voltammetry (e), Nyquist plots (f) and J-V characteristics (g) of DSSCs under front illumination. (Reproduced with the permission from Ref. [146], Copyright 2017 Elsevier)**

A. Ali et al. modified highly aligned MWCNTs fiber composite and starting from it they subsequently fabricated a CE through a simple dip coating method to be applied in DSSC [147]. Modified MWCNTs based CE exhibited a noticeable improvement in catalytic performance in comparison to the pristine MWCNTs fiber electrode and led to an overall conversion efficiency of 5.03%, slightly higher than that obtained in presence of a traditional Pt electrode. Good photovoltaic performance even after bending up to 90° was also successfully obtained.

Composites of MWCNTs were also prepared utilizing other polymers such as poly(diallyldimethylammonium chloride) (PDDA),, PPy, PANI and polythiophene (PTh). X. Mao et al. [148] prepared MWCNTs-poly(diallyldimethylammonium chloride) (PDDA) composite based CE through spin coating technique . MWCNTs were first purified with $HNO_3$, then PDDA was mixed in presence of sodium chloride solution in a separated flask and finally the composite was coated on FTO glass with a final thickness up to 30 μm. Results revealed

that PDDA/MWCNTs electrode exhibited reduced charge transport hindrance and high electrocatalytic activity, which led to a noticeable conversion efficiency of 5.66%.

MWCNTs-polypyrrole (PPy) composites were fabricated and employed as DSSCs CE by Hou et al. (see **Fig. 11**). The MWCNTs were spin-coated on conducting glass, while the PPy was electrodeposited on MWCNT layer by means of a CVD technique. An excellent photoconversion efficiency of 7.15% was obtained, that can be attributed to the enhanced catalytic activity due to the presence of PPy [149].

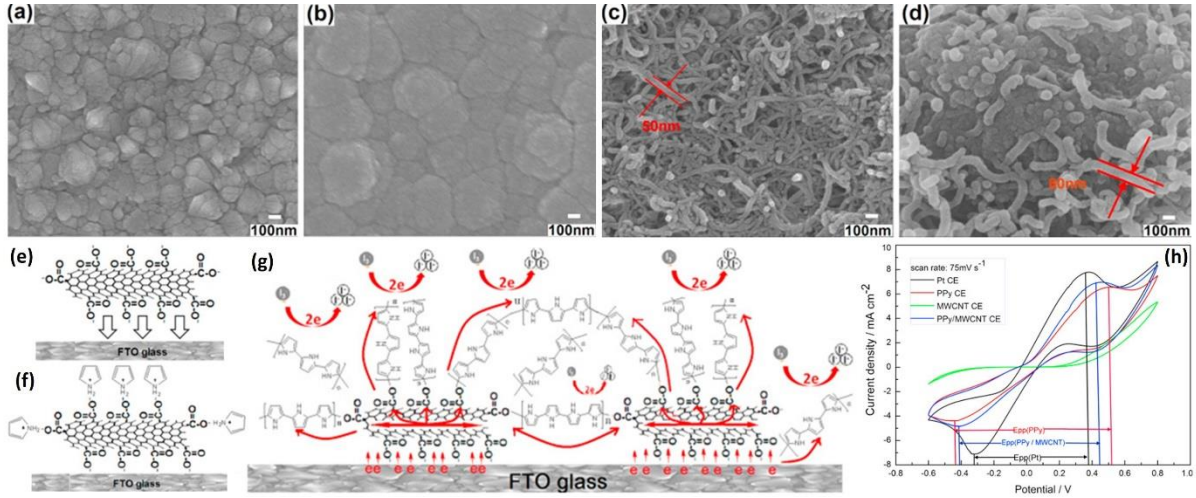


**Fig. 11. SEM images of the bare FTO (a), PPy (b), MWCNTs (c), and PPy/MWCNT (d) based CEs. Schematic diagram of the MWCNTs preparing on the FTO substrate (e), Pyrrole monomer absorbing on the surface of the MWCNTs (f), catalytic mechanism of PPy onto the MWCNTs and FTO substrate (g), cyclic voltammetry at a scan rate of 75 mV $s^{-1}$ (h). (Reproduced with the permission from Ref. [149], Copyright 2016 Elsevier)**

Recently, Li et al. synthesized honeycomb PPy using sacrificial template method. PMMA was deposited by spin coating technique over an acid functionalized MWCNTs-FTO substrate followed by dissolution in chloroform solvent after electrodeposition of PPy [150]. The obtained CE was applied in bifacial DSSCs. The efficiencies for front and rare illuminations were 7.07 and 4.11%, respectively, which were higher than that obtained with flat PPy.

Furthermore, Kuliček et al. synthesized PPy-MWCNTs based CEs using electro polymerization technique using different surfactants and achieved an efficiency of 2.89% when sodium dodecylbenzenesulfonate (DBSNa) was employed [151].

Blends consisting of MWCNTs, poly(3-hexylthiophene) (P3HT) and PPy were successfully synthesized by radiofrequency (RF)-rotating plasma polymerization method to act as CEs of DSSCs [152]. Pure MWCNTs exhibited a tube-shaped permeable structure. On the other hand, composite films showed disordered granulated structure. Results displayed that the P3HT/MWCNTs cell showed an efficiency of 1.24%, whereas the PPy/MWCNTs based one exhibited an efficiency of 0.80%. Composites of MWCNTs and different conductive polymers such as PEDOT, PANI and polythiophene (PTh) were effectively synthesized via radiofrequency (RF)-rotating plasma grafting technique to play the role of CEs in DSSCs. These latter revealed efficiencies of 2.07, 1.61 and 1.32% when using PANI/MWCNTs, PTh/MWCNTs and PEDOT/CNTs based CEs, respectively. These results highlight the highest catalytic activity for PANI polymer, thus resulting in a higher efficiency [153].

**Tab.** 2 details the main characteristics and the photovoltaic efficiencies of DSSCs based on CNTs-polymer composites based CEs.

**Tab. 2. Main features and photovoltaic performance of DSSCs fabricated with CNTs-polymer composites based CE**

| No. | CE Material | Deposition method | Photoanode | Sensitizer | Redox couple | PCE (%) | PCE vs Pt (%) | Ref. |
|---|---|---|---|---|---|---|---|---|
| 1 | SWCNTs<br>SWCNTs-PVP (1%) | Simple casting | $TiO_2$ | N719 | $I_3^-/I^-$ | 2.4<br>4.5 | n.a. | [137] |
| 2 | PPy<br>PPy-SWCNTs(2%) | In-situ polymerization over FTO | $TiO_2$ | N719 | $I_3^-/I^-$ | 6.03<br>8.30 | n.a. | [139] |
| 3 | PEDOT<br>PEDOT-MWCNTs (0.6%) | Spin coating | $TiO_2$ | N3 | $I_3^-/I^-$ | 7.44<br>7.77 | 8.08 | [140] |
| 4 | MWCNTs<br>PEDOT<br>MWCNTs-PEDOT | Simple casting | $TiO_2$ | N719 | $I_3^-/I^-$ | 3.88<br>4.32<br>4.62 | n.a. | [141] |
| 5 | PEDOT<br>PEDOT-MWCNTs | Spin coating and electrodeposition | $TiO_2$ | N719 | $I_3^-/I^-$ | 7.51<br>9.07 | 7.71 | [146] |
| 6 | PSSA-MWCNTs<br>PEDOT:PSS-MWCNTs | Spin coating | $TiO_2$ | N719 | $I_3^-/I^-$ | 3.6<br>6.5 | 8.5 | [142] |

| | | | | | | | | |
|---|---|---|---|---|---|---|---|---|
| 7 | PEDOT:PSS-MWCNTs | Spin coating | $TiO_2$ | N719 | $I_3^-/I^-$ | 6.1 | n.a. | [143] |
| 8 | ACNTs<br>ACNTs-PEDOT:PSS<br>ACNTs-Triton-X100<br>ACNTs-Both | Doctor blading | $TiO_2$ | N719 | $I_3^-/I^-$ | 2.96<br>3.85<br>3.22<br>3.58 | n.a. | [144] |
| 9 | MWCNT-10%<br>MWCNT-HSPM (10/5%) | Screen printing | $TiO_2$ | N719 | $I_3^-/I^-$ | 5.69<br>5.94 | 7.15 | [145] |
| 10 | AMWCNTs fiber<br>PEDOT:PSS modified MWCNTs fibers | Dip coating | $TiO_2$ | N719 | $I_3^-/I^-$ | 2.79<br>5.03 | 4.98 | [147] |
| 11 | PPy<br>MWCNT<br>PPy-MWCNTs | Spin coating and electrodeposition | $TiO_2$ | N719 | $I_3^-/I^-$ | 5.72<br>1.72<br>7.15 | 7.76 | [149] |
| 12 | P3HT-MWCNT<br>PPy-MWCNT | RF rotating plasma | $TiO_2$ | Z907 | $I_3^-/I^-$ | 1.24<br>0.80 | n.a. | [152] |
| 13 | PANI-MWCNTs<br>P3HT-MWCNTs<br>PEDOT-MWCNTs | RF rotating plasma | $TiO_2$ | Z907 | $I_3^-/I^-$ | 2.07<br>1.61<br>1.32 | | [153] |

| | | | | | | | | |
|---|---|---|---|---|---|---|---|---|
| 14 | MWCNTs<br>PDDA-MWCNTs | Spin coating | $TiO_2$ | N719 | $I_3^-/I^-$ | 4.48<br>5.66 | 6.73 | [148] |
| 16 | flat-PPy<br>MWCNTs-f-PPy<br>honeycomb-PPy<br>MWCNTs-h-PPy | Spin coating and electrodeposition | $TiO_2$ | N719 | $I_3^-/I^-$ | 5.78<br>6.18<br>6.32<br>7.07 | n.a. | [150] |
| 17 | MWCNTs<br>PPy-DBSNa<br>PPy-MWCNTs-DBSNa | Doctor blading and electropolymerisation | $TiO_2$ | N719 | $I_3^-/I^-$ | 2.50<br>2.75<br>2.89 | 4.92 | [151] |

### 4.3 Metal oxides, sulfides, nitrides & phosphides composites based CEs

Transition metal compounds commonly show high catalytic activity but suffer from low conductivity. To overcome this drawback, they are employed in combination with other conductive materials for the fabrication of DSSC CEs. Due to their high conductivity, CNTs are a promising material to be incorporated in metal oxides to enhance the cell performance. A number of metal compounds are used for the above-mentioned application. The most common are nickel oxide (NiO) [154], tungsten oxide ($WO_2$) [155], lanthanum oxide ($La_2O_3$), nickel sulfide (NiS) [156], cobalt sulfide (CoS) [157], tungsten sulfide ($WS_2$) [158], molybdenum sulfide (MoS) [159], vanadium sulfide ($VS_2$) and bismuth sulfide ($Bi_2S_3$).

Metal sulfide-CNTs composites based CE materials were developed by L. Zhang et al. by using a solution based method, and a device efficiency value of 3.13% was obtained for CoS/CNTs. Other different CEs based on Pt/FTO, Pt/CNTs and NiS/CNTs composites were also prepared, and their performance was compared to each other. The better performance exhibited by the CoS/CNTs based CE arises from the homogenous deposition of the CoS nanoparticles [160].

Wu et al. fabricated a CE based on glucose aided $WS_2$-MWCNTs hybrid by hydrothermal process and gained an efficiency of 7.36% [158]. Doctor blade technique was used for the preparation of the CE. The as-prepared CE exhibited higher surface area and decreased charge transport resistance, which were responsible for an improved catalytic activity comparable to that showed by the Pt reference electrode. Due to promising results shown by tungsten sulfide, other group members combined with CNTs were also studied as CE materials for DSSCs. Tai et al. fabricated MWCNTs-$MoS_2$ nanocomposite and used it as CE in DSSCs [161]. The synthesis of the catalyst was carried out via simple blending of $MoS_2$ and MWCNTs into an acidic solution followed by the transformation of the compact intermediate into MWCNT-$MoS_2$ nanocomposite at an elevated temperature of 650°C in Hydrogen flow. The prepared CE revealed an enhanced efficiency of 6.45%, analogous to the 6.41% shown by Pt CE.

Recently, Theerthagiri et al. developed flower-like $MoS_2$ microspheres by using hydrothermal technique that were subsequently mixed with different carbon based materials in order to increase their conductivity. An efficiency as high as 3.17% was reached with the carbon nanofibers based CE, followed by the one based on MWCNTs (3.08%) [162].

Lu et al. [163] prepared various DSSCs CE materials, namely Pt, nickel sulfide, MWCNTs and nickel sulfide/MWCNTs composite, through hydrothermal method and subsequently analyzed their photovoltaic performance (see Fig. 12). The highest efficiency of 6.87% was achieved with the nickel sulfide/MWCNTs composite. This value resulted to be higher than the ones obtained with MWCNTs and nickel sulfide electrodes taken individually and almost equivalent to the one attained with Pt based CE. Theerthagiri et al. suggested NiS-MWCNTs composite could also be used as cost-effective CE for the fabrication of Pt-free DSSCs [164].

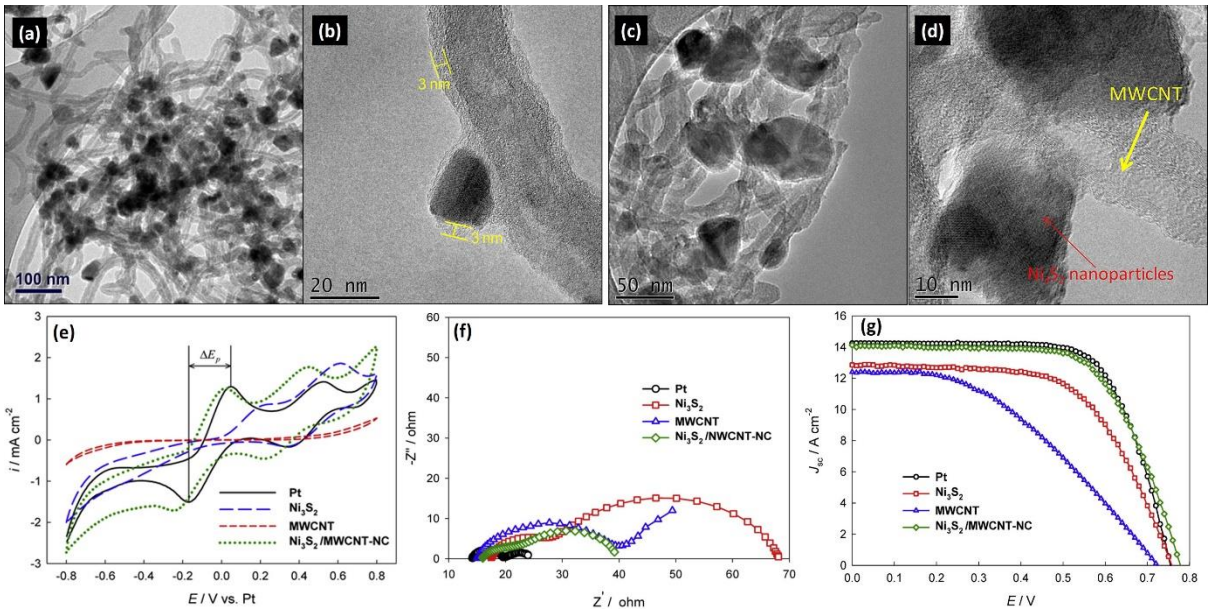


**Fig. 12. HR-TEM images of un-annealed (a and b), and annealed (c and d) $Ni_3S_2$/MWCNT-NCs. CV curves of $I_2/I_3^-$ system (e), Nyquist plots (f), J-V curves (g) of the symmetrical DSSCs assembled with the Pt, $Ni_3S_2$, MWCNT and $Ni_3S_2$/MWCNT-NC CEs. (Reproduced with the permission from Ref. [163], Copyright 2014 Elsevier)**

Vanadium sulfide/ MWCNTs composites were also employed as CE for DSSCs by Yue et al. They used an in situ hydrothermal technique for the fabrication of the composite material and doctor blade technique for coating the material over FTO. A promising efficiency of 8.02%, far higher than that obtained by using a Pt based CE (6.49%), was achieved because of high catalytic activity at the electrode/electrolyte interface [165]. The CNTs content was 0.05% and the hydrothermal temperature was fixed to 180°C during the synthesis.

Tai et al. synthesized nanocomposites constituted of carbon nanotubes and cobalt sulfide in two different forms, i.e. CNT@$Co_9S_8$ and CNT@$CoS_{1.097}$. Both of the forms were prepared on a conducting glass substrate with the help of simple and straightforward spray coating technique and then annealed in nitrogen atmosphere at 400°C and 600°C, respectively [166]. Despite its comparatively lower surface area, the CNT@$Co_9S_8$ CE displayed improved electrocatalytic performance as compared to CNT@$CoS_{1.097}$ based CE. As a result, CNT@$Co_9S_8$ CE based DSSCs exhibited a noticeable efficiency of 7.78%, which was greater than that obtained with CNT@$CoS_{1.097}$ nanocomposite CE based (7.29%) and Pt based CE (7.46%).

Memon et al. prepared a $Bi_2S_3$-MWCNTs composite based CE by tape casting over FTO substrate and employed it in quasi-solid state DSSCs. The hetero-materials were mixed in different ratios and a highest efficiency of 8.24%, comparable to that achieved with Pt CE (8.47%), was obtained when MWCNTs were kept at 0.8 wt% [167]. Furthermore, CuS-MWCNTs composite in different ratios were prepared by Zhang et al. and deposited over FTO to be used as CEs in quasi-solid state DSSCs. A maximum photo-conversion efficiency of 5.254% (Pt based CE DSSC efficiency = 2.680%) was achieved when CuS content was kept at 100 wt%. The better photovoltaic performance of the above mentioned electrode with respect to the standard Pt based one was attributed to its greater catalytic activity and lower charge transfer resistance [168]. Similarly, Lin et al. prepared a CoS-MWCNTs composite based CE

for application in DSSCs. MWCNTs were oxidized and deposited over FTO through electrophoresis followed by cathodic deposition of CoS (see **Fig. 13**). The DSSC made with such CE delivered an efficiency of 6.96%, which was higher than the one achieved in presence of a Pt-Sputtered CE (5.99%) [169].

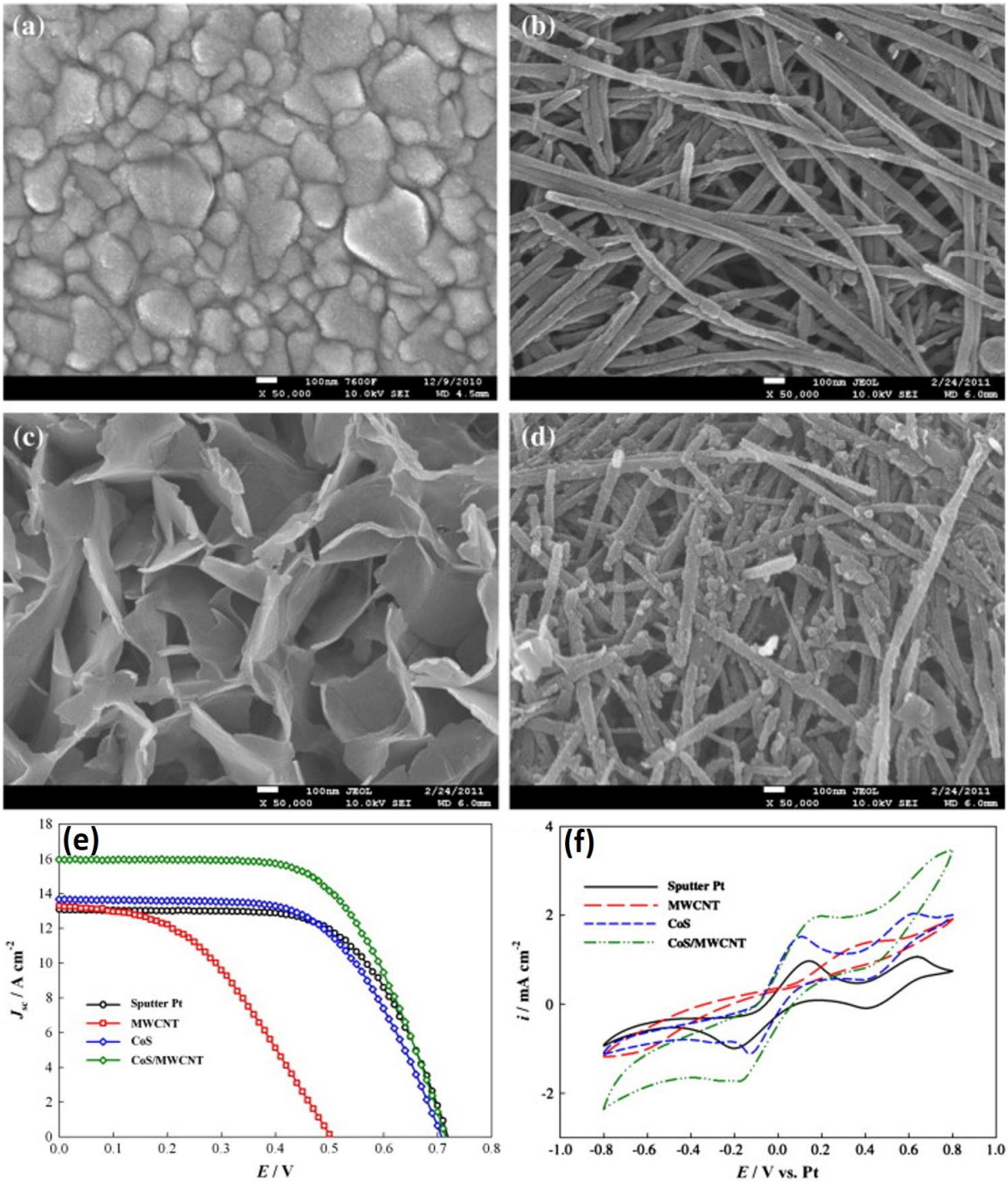

**Fig. 13. SEM images of various thin film materials; a). Sputtered Pt, b). MWCNTs, c). CoS, and d). CoS/MWCNT, e) J-V characteristics, and f) CV at a scan rate of 10 $mVs^{-1}$ of DSSCs based on sputtered-Pt, MWCNTs, CoS, and CoS/MWCNTs CEs. (Reproduced with the permission from Ref. [169], Copyright 2011 Elsevier)**

Recently, compounds that were previously rarely investigated such as $La_2O_3$, $Bi_2S_3$ and CuS were employed as CE layer for DSSCs in combination with MWCNTs. Wu et al. prepared various $La_2O_3$-MWCNTs based composites and employed them in DSSCs as CE. $La_2O_3$ was synthesized through solid phase reaction followed by mixing with MWCNTs in different ratios, i.e. 5:1, 3:1 and 1:1, by ball milling. The as-obtained composite was finally spray coated over FTO substrate and a maximum efficiency of 5.20% was achieved when the $La_2O_3$-MWCNTs ratio was kept at 5:1. The photo-conversion efficiency of all the prepared composites was higher than the one showed by the Pt based electrode (4.54%) [170].

The synthesis of a CE based on the composite of MWCNTs and nickel oxide (NiO) using a simple hydrothermal method was performed by Al-bahrani et al. [171] (see **Fig. 14**) . The NiO nanofilament (NF) coated on the MWCNTs was verified through various structural and morphological techniques. The NiO-NF/MWCNTs composite showed high catalytic activity because of high surface area and low charge transfer resistance at the interface between the CE and the electrolyte. When employing it in a DSSC, an efficiency of 7.63% was achieved, which is higher than that showed by the Pt counterpart (6.72%).

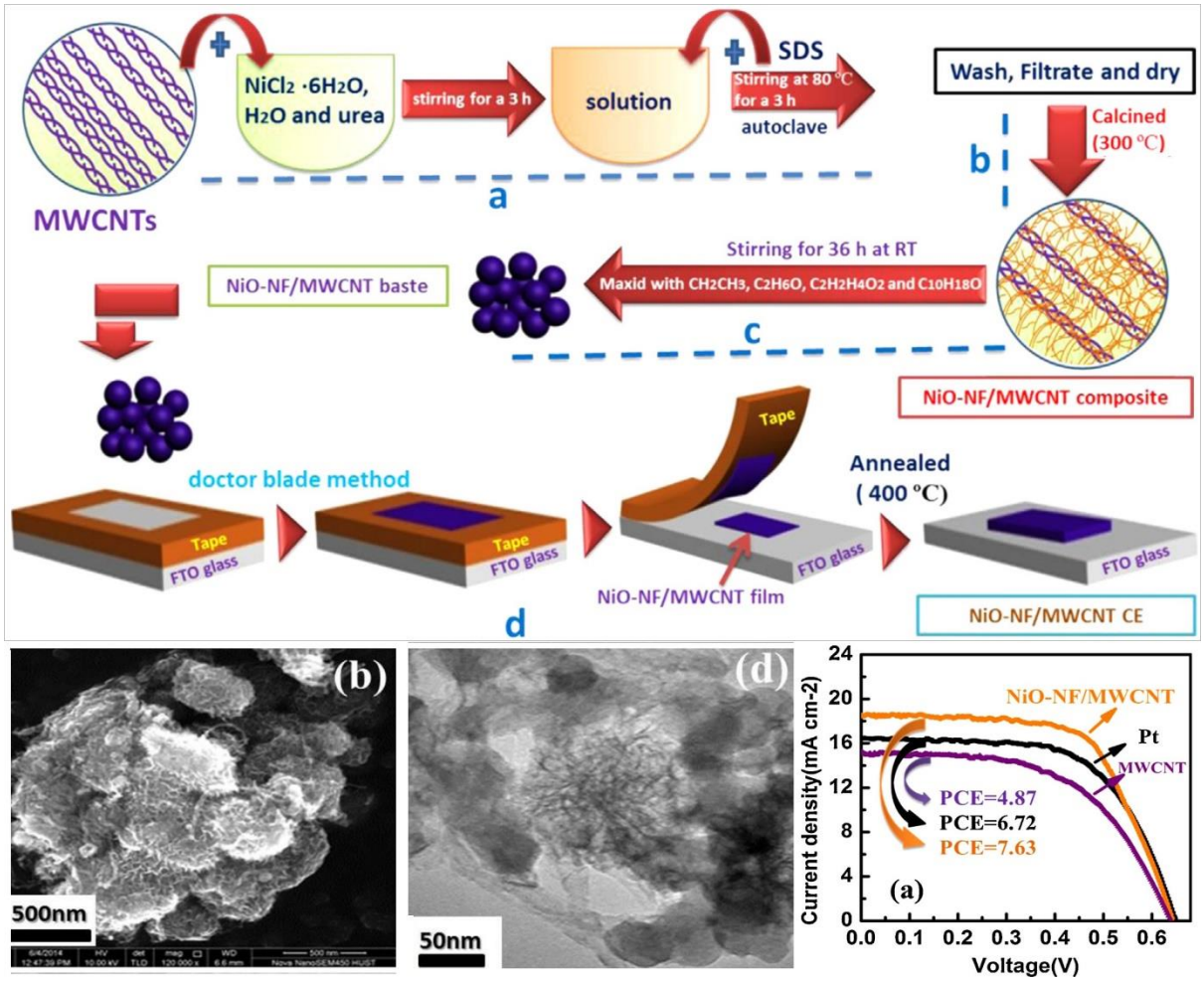


**Fig. 14. Schematic illustration of the preparation of NiO-NF/MWCNT CE (a), SEM and TEM images of NiO-NF/MWCNT composite (b), J-V characteristics of the Pt, NiO-NF/MWCNT, MWCNT and NiO-CE (c). (Reproduced with the permission from Ref [171], Copyright 2015 Elsevier)**

**Tab 3** reports the main characteristics and the photovoltaic performance of DSSCs fabricated with CNTs-metal oxides and sulfides composites based CEs.

**Tab 3. Main features and photovoltaic performance of DSSCs assembled with CNTs-metal oxides and sulfides based CEs.**

| No. | CE Material | Deposition method | Photoanode | Sensitizer | Redox couple | PCE (%) | PCE vs Pt (%) | Ref. |
|---|---|---|---|---|---|---|---|---|
| 1 | $WS_2$<br>MWCNTs<br>(G-A)$WS_2$-MWCNTs | Doctor blading | $TiO_2$ | N719 | $I_3^-/I^-$ | 5.32<br>4.34<br>7.36 | 7.54 | [158] |
| 2 | $MoS_2$<br>MWCNTs<br>MWCNTs-$MoS_2$ | Drop casting | $TiO_2$ | N719 | $I_3^-/I^-$ | 4.99<br>3.53<br>6.45 | 6.41 | [161] |
| 3 | $MoS_2$<br>$MoS_2$-MWCNTs | Doctor blading | $TiO_2$ | N3 | $I_3^-/I^-$ | 1.04<br>3.08 | n.a. | [162] |
| 4 | $VS_2$<br>$VS_2$-CNTs | Doctor blading | $TiO_2$ | N719 | $I_3^-/I^-$ | 6.49<br>8.02 | 6.49 | [165] |
| 5 | $Ni_2S_3$<br>MWCNTs<br>$Ni_2S_3$-MWCNTs | Doctor blading | $TiO_2$ | N719 | $I_3^-/I^-$ | 5.77<br>3.76<br>6.87 | 7.24 | [163] |
| 6 | CoS<br>MWCNTs<br>CoS-MWCNTs | Electrophoresis and electrodeposition | $TiO_2$ | N719 | $I_3^-/I^-$ | 6.96<br>2.91<br>5.86 | 5.99 | [169] |

| | | | | | | | | |
|---|---|---|---|---|---|---|---|---|
| 7 | MWCNTs-$CoS_{1.097}$<br>MWCNTs-$Co_9S_8$ | Spray coating | $TiO_2$ | N719 | $I_3^-/I^-$ | 7.29<br>7.78 | 7.46 | [166] |
| 8 | $La_2O_3$<br>MWCNTs<br>$La_2O_3$-MWCNTs (5:1) | Spray coating | $TiO_2$ | N719 | $I_3^-/I^-$ | 0.77<br>3.94<br>5.20 | 4.54 | [170] |
| 9 | $Bi_2S_3$<br>MWCNTs<br>$Bi_2S_3$-MWCNTs (0.8) | Tape casting method | $TiO_2$ | N719 | $I_3^-/I^-$ | 4.51<br>6.82<br>8.24 | 8.47 | [167] |
| 10 | MWCNTs<br>100% CuS-MWCNTs | Doctor blade technique | $TiO_2$/ RGO | ZnS and CdS | $S^{2-}/S_n^{2-}$ | 2.577<br>5.254 | 2.680 | [168] |
| 11 | MWCNTs<br>NiO-NF-MWCNTs | Doctor blading | $TiO_2$ | N719 | $I_3^-/I^-$ | 4.87<br>7.63 | 6.72 | [171] |

## 4.4 Doped and metal coated CNTs based CEs

CNTs are one of the most important and easily available dopable materials for the manufacturing of DSSC CEs, and different materials can be used for their doping. The effect of the CNTs doping in CEs fabrication can be studied in terms of catalytic behavior, stability, and efficiency. Tantang et al. developed a Pt-free CE for DSSC by air spraying MWCNTs over a quartz glass followed by spraying of a layer of N-doped MWCNTs. The electrode showed a good transparency of 57% at 550 nm and allowed achieving a DSSC photo-conversion efficiency of 2.18%. The good performance displayed by the Pt-free CE was attributed to the good catalytic activity of the N-doped CNTs and the high conductivity of the bare CNTs [172].

Pod-like nitrogen (N)-doped carbon nanotubes with encapsulated FeNi alloy nanoparticles were synthesized via $Ni_2Fe(CN)_6$ direct pyrolysis in an inert atmosphere. CEs attained by this process are environmental friendly, non-toxic, in-expensive and extremely competent [173]. The Pod(N)-FeNi catalyst demonstrated excellent electrocatalytic activity, low peak separation among the anodic and cathodic peaks, low charge diffusion resistance, higher exchange current density and enhanced electrochemical stability under extended cycling with respect to that of sputtered Pt electrode. The DSSCs employing the Pod(N)-FeNi as the CE showed an overall efficiency of 8.82%, higher than that of the sputtered Pt CE (8.01%) (see Fig. 15). Nevertheless, the incapsulated FeNi nanoparticles themselves did not show good catalytic activity, therefore other metals which are able to interact differently with CNTs imparting them significantly different properties have been explored. Therefore, they further incorporated Ni and Co metal nanoparticles into N-doped MWCNTs, which revealed good electrocatalytic performance and made possible to achieve efficiencies in DSSC up to 8.39 and 7.75%, respectively.

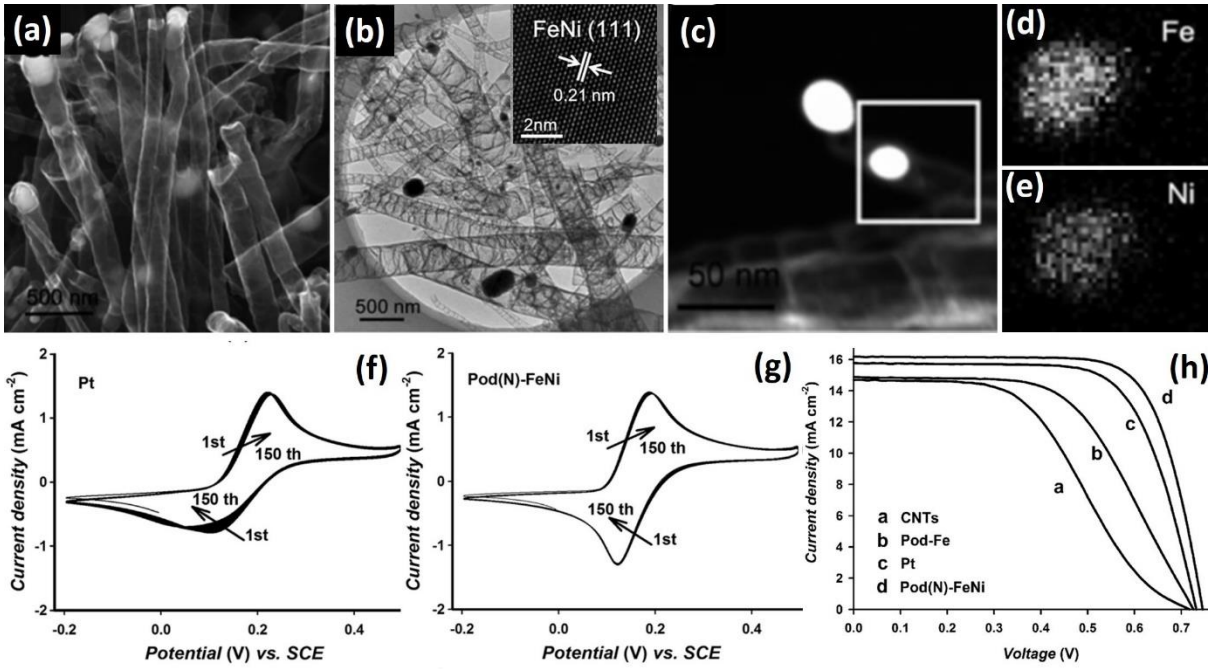


**Fig. 15. SEM image (a), TEM image (b) of the Pod (N)-FeNi (inset: HRTEM image of the FeNi alloy nanoparticle). HRTEM image (c), and elemental mapping of Fe (d) and Ni (e) elements in the metal NPs in boxed area of (c). Sequential cyclic voltammograms for Pod(N)-FeNi (f) and d sputtered Pt CEs (g). J-V curves of the DSSCs using CNTs, Pod-Fe, Pt, and Pod(N)-FeNi as CEs. (Reproduced with the permission from Ref. [173], Copyright 2014 Wiley-VCH )**

Shrestha et al. [174] used polydopamine (PDA) to generate catalytically active nitrogen doped carbon materials ($CN_x$) on MWCNTs. The as-prepared composites were employed as CEs in DSSCS and an efficiency of 7.3%, which was slightly higher than the one obtained with a Pt based electrode (7.1%), was achieved for the optimized material containing PDA/CNT ratio of 2:1 and annealed at 800°C.

Similarly, Chen et al. synthesized Ni encapsulated N-doped MWCNTs by facile thermal decomposition method and evaluated them as CE material in DSSCs (see **Fig.16**). An efficiency of 8.94%, which was higher than the one delivered by Pt based CE (7.53%), was

obtained and attributed to the homogeneously distributed Ni-C interfaces, porous structure with various defects, good electrical conductivity as well as corrosion resistance [175].

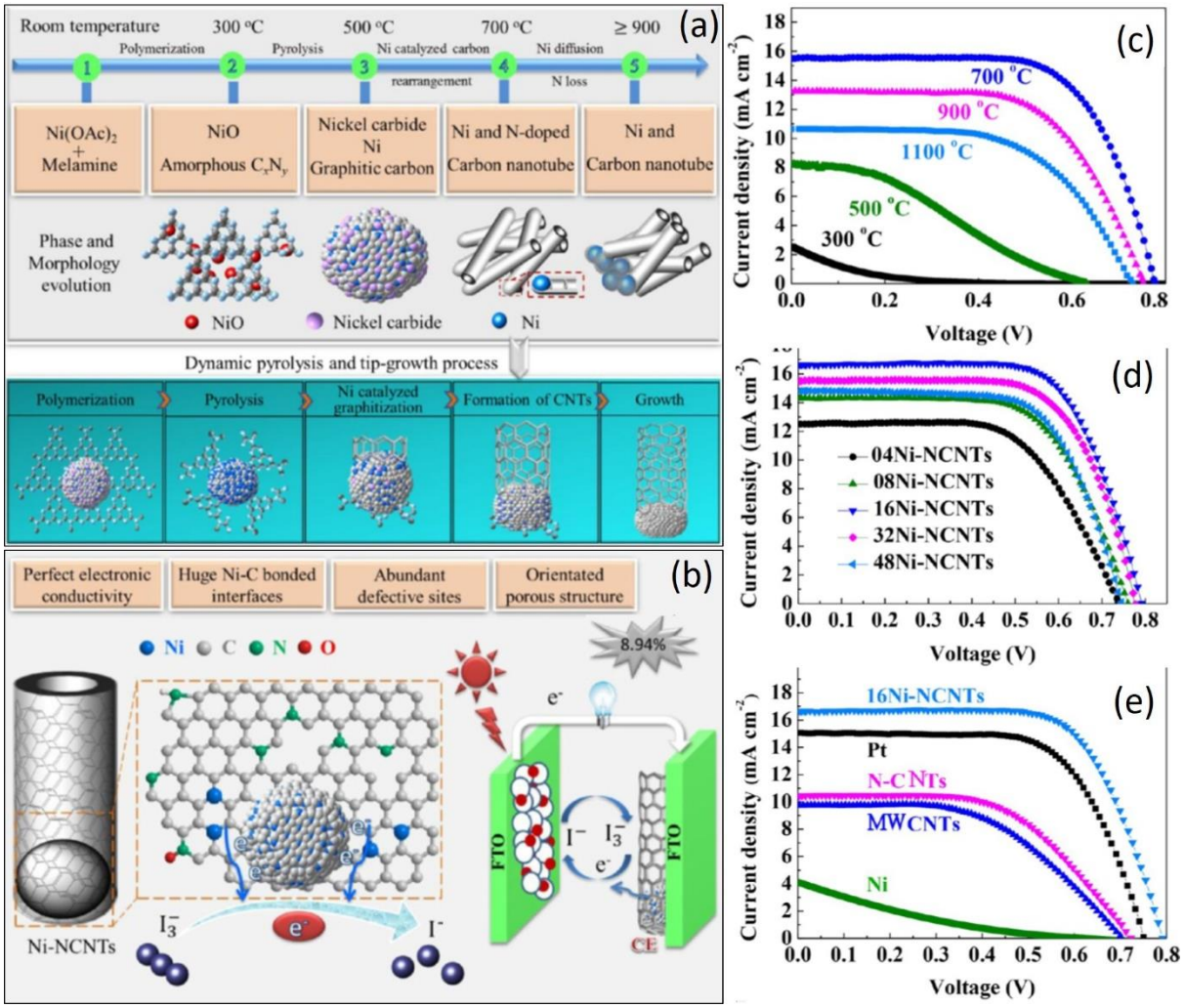


**Fig.16 Scehmatic of mechanism of synthesis for preparation of Ni- and N-doped-CNT (a), Schematic layout of electrocatalytic activity of the Ni-NCNT CE(b), J-V curves of NiNC-x (c), yNi-NCNTs (d) and reference-CE-based DSSCs (d). (Reproduced with the permission from Ref. [175], Copyright 2017 American Chemical Society).**

Furthermore, Ou et al. embedded Co nanoparticles in N-doped MWCNTs by using one-step pyrolysis of ZIF-67 metal organic framework under hydrogen atmosphere (see **Fig. 17**). The composite was then spin coated over FTO and the as-obtained film was applied as a CE in a

DSSC. An efficiency of 8.18%, which was higher than that exhibited by a standard Pt based CE (7.54%), was achieved and ascribed to the excellent catalytic activity [176].

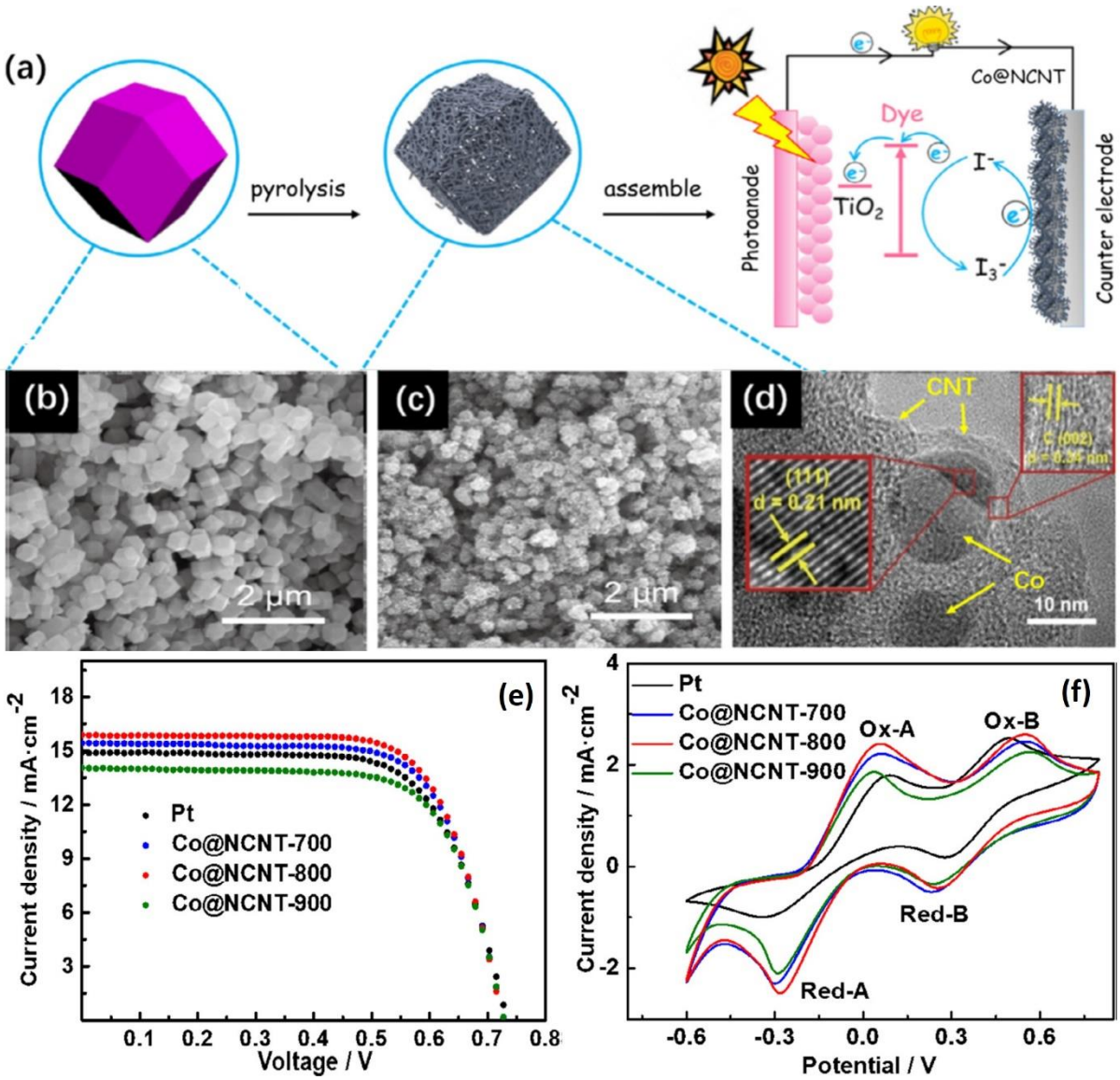


**Fig. 17 Schematic diagram of fabrication process of Co@NCNT CE materials for DSSCs (a). SEM image of ZIF-67 (b) SEM image and (c) TEM image (d) of Co@ NCNT-800. J-V curves Co@NCNT and Pt as CEs (e) CV curves of $I^-/I^{-3}$ redox couple on Co@NCNT CEs and Pt CE at a scan rate of 50 mV $s^{-1}$ (Reproduced with the permission from the Ref. [176], Copyright 2018 Elsevier)**

Lee et al. prepared arrays of vertically aligned N-doped MWCNTs which were readily transferred to glass or plastic substrates and used as CEs in DSSCs. The efficiency achieved

was 7.04%, which was comparable to that showed by the Pt based CE (7.34%). This outstanding performance was attributed to the vertical alignment, which provides large surface area, and to the electron rich nitrogen doping, which increases the catalytic activity as well as the conductivity [177].

Beside nitrogen, other heteroatoms are commonly adopted to dope CNTs. Among them, one of the most promising is boron (B), which is an electron deficient atom and therefore it is able to modify the chemically inert $sp^2$ carbon structure, thus resulting in a large number of free-flowing $\pi$ electrons. Leu et al. synthesized B-doped MWCNTs and drop casted them on FTO slices to prepare CEs for the fabrication of DSSCs. They annealed the prepared CEs at different temperatures and the highest efficiency (7.91%) was achieved when the annealing temperature was kept to 500°C. The noticeable efficiency, which was comparable to the one delivered by the counterpart Pt based electrode (8.03%), was attributed to the higher catalytic activity and conductivity achieved at that annealing temperature [178]. Similarly, Yeh et al. prepared B-doped MWCNTs based electrodes using various concentrations of boron and used them as electrocatalysts for DSSCs. The highest efficiency of 7.17%, comparable to that showed by the Pt based electrode (7.98%), was obtained when the doping concentration was 0.04% and attributed to the higher catalytic activity and conductivity [179].

Arbab et al. synthesized activated charcoal (AC)-doped MWCNTs by using an enzymatic dispersion method. Charcoal was obtained from different sources, i.e. coal, coconut shell and pine tree. A porous morphology was highlighted, which allowed obtaining a high surface area and a defect-rich structure responsible for a greater catalytic activity and a lower charge transport resistance. The composite material was employed as CE in quasi-solid state DSSCs and an efficiency of 10.07%, higher than that showed by the Pt based electrode, was achieved in presence of pine tree derived charcoal at a concentration of 0.8% [180].

Metal coated and decorated CNTs have also been used as counter electrode materials for DSSCs. Ruthenium (Ru) coated MWCNT was investigated by Han et al. as a metal-free alternative CE material for DSSCs [181]. Purified MWCNT was sprayed onto FTO conductive glass substrate and subsequently 30 nm-thick Ru crystalline thin films were coated on a MWCNT template at low temperature by atomic layer deposition (ALD) using RuDi (isopropyl-methylbenzene-cyclohexadiene Ru) and $O_2$ as precursors. As evidenced by morphological analysis, the effective surface of the CE increased linearly as both the amount of sprayed MWCNT and the conformity of the Ru coating around the MWCNT nanotemplate enhanced. Moreover, the photo-conversion efficiency of the DSSC increased up to 3.3% as the amount of MWCNT raised.

Lu et al. [182] effectively applied N,S doped hollow core shell carbon microspheres (N,S-HCCS) as the CE for DSSCs. The photo conversion efficiency (PCE) of the cell reaches to 8.03%, which is far larger than the Pt's value 7.2%. The more high adsorption of electrons due to large surface area and three dimensional sphere structure of (N,S-HCCS) may be the reason for outstanding catalytic performance exhibited by this electrode. Similarly, the fabrication of CEs by combining SWCNTs spray coating and chloroplatinic acid (source of Pt nanoparticles) chemical reduction along with formic acid was also carried out by Kim et al. [183]. Thanks to the presence of Pt nanoparticles, the catalytic activity for triiodide reduction enhanced, thus leading to a noticeable DSSC photo-conversion efficiency as high as 5.11%.

Arbab et al. synthesized organic N-doped MWCNTs using an organic compound named serum bovine albumin (cBSA) protein complex, which upon cationization releases huge number of activated nitrogen acting as a dopant source. The prepared material, when used as CE in DSSCs, gave a promising efficiency of 9.55%, which is comparable to the one exhibited by the Pt based CE (9.89%). This excellent performance was attributed to the high charge polarization

due to the electronegativity difference and to the structural strain caused by the presence of the organic compound [184].

**Tab.** 4 summarizes the main characteristics and the photovoltaic performance of DSSCs fabricated with doped CNTs based CEs.

**Tab. 4. Main characteristics and photovoltaic performance of DSSCs fabricated with doped CEs**

| No. | CE Material | Deposition method | Photoanode | Sensitizer | Redox couple | PCE (%) | PCE vs Pt (%) | Ref. |
|---|---|---|---|---|---|---|---|---|
| 1 | Bi-layer MWCNTs-NMWCNTs | Spray coating | $TiO_2$ | N719 | $I_3^-/I^-$ | 2.18 | 3.95 | [172] |
| 2 | NMWCNTs<br>NMWCNTs-FeNi | Spray coating | $TiO_2$ | N719 | $I_3^-/I^-$ | 4.87<br>8.82 | 8.01 | [173] |
| 3 | NMWCNTs<br>NMWCNTs-Ni | Direct coating | $TiO_2$ | N719 | $I_3^-/I^-$ | 4.24<br>8.94 | 7.53 | [175] |
| 4 | NMWCNT-Co | Spin coating | $TiO_2$ | N719 | $I_3^-/I^-$ | 8.18 | 7.54 | [176] |
| 6 | MWCNTs-400<br>BMWCNTs-500 | Drop casting | $TiO_2$ | N719 | $I_3^-/I^-$ | 6.02<br>7.91 | 8.03 | [178] |
| 7 | MWCNTs<br>BMWCNTs | Drop coating | $TiO_2$ | N719 | $I_3^-/I^-$ | 5.98<br>7.17 | 7.98 | [179] |
| 8 | MWCNTs<br>ACMWCNTs-0.8% | Tape casting | $TiO_2$ | D719 | $I_3^-/I^-$ | 7.16<br>10.05 | 9.30 | [180] |

| | | | | | | | | |
|---|---|---|---|---|---|---|---|---|
| 9 | NMWCNT-Co<br>NMWCNT-Ni | Spray coating | $TiO_2$ | N719 | $I_3^-/I^-$ | 7.75<br>8.39 | 7.67 | [185] |
| 10 | MWCNTs<br>N-$CN_x$/MWCNTs | Doctor blading | $TiO_2$ | N719 | $I_3^-/I^-$ | 4.48<br>7.38 | 7.13 | [174] |

## 4.5 CEs based on hybrid composite materials

The composites of CNTs with other organic and inorganic materials have also been used as CEs for DSSCs. Beside this, the combination of CNTs with various other carbon nanomaterials particularly graphene related materials has also been proven to be a potential candidate for CEs. For instance, three different CEs for DSSCs based on graphene, SWCNTs and SWCNTs/graphene composites were synthesized by electrophoretic deposition technique by Kim et al. [186]. The electrochemical and optical characteristics of the carbon based CEs were examined by different characterization techniques. The highest power conversion efficiency of 5.87% was achieved with the graphene based CE, closely followed by the composite sample with an efficiency of 5.17%.

Similarly, a hybrid material consisting of MWCNTs and graphene was prepared through solution-based method and employed as a CE, leading to an overall device efficiency of 4.66%. Hybrid electrodes show a number of benefits compared to other CEs made of graphene or platinum films, comprising a lower internal resistance, a higher rate of charge transport and a lower electron lifetime. The film thickness noticeably affects the overall performance of the cell. In particular, an increase in the film thickness led to the rise of the overall device efficiency, due to the simultaneous increase of fill factor, voltage, and current density. Based on efficiency, stability and cost aspects, this hybrid electrode can be regarded as a suitable alternative material to Pt for the CE of DSSCs [187].

Three dimensional nitrogen doped graphene/reduced hydroxylated CNTs composite aerogel (NG/CNT-OH) was developed through a two-steps hydrothermal reaction using hydroxylated carbon nanotubes (CNTs-OH) and graphene oxide (GO) as reactants [188]. NG/CNT-OH composite aerogel exhibited excellent electrocatalytic performances for triiodide/iodide redox couple, mainly attributed to its hierarchical porosity structure with large numbers of exposed active edge sites, which provide the efficient pathways of electrons and ions transport. The as

prepared NG/CNT-OH composite aerogel was then compressed to form carbon paper and was used as flexible and economical TCO-free CE for DSSCs. The fabricated CE showed excellent carrier transport ability, high electrocatalytic activity, and exceptional mechanical flexibility. The DSSCs assembled with the optimized NG/CNT-OH CE achieved a noticeable power conversion efficiency value of 6.36%, higher in comparison to those obtained by Pt CE based DSSCs in similar conditions (5.74%).

The brick-like three-dimensional graphene-CNTs with N-doping (NGC) nanocomposites having several upright active edge points and outstanding electrochemical catalytic activity were synthesized by mechanically grinding the GO-CNTs filtration films as proposed by Ma et al. as CEs for DSSC [189]. The dimension and concentration of N-doping (breaking particles) were tuned via varying the altered ratio of graphene to CNTs. The fabricated CEs allowed achieving a DSSC maximum photo conversion efficiency of 6.74 %, quite close to that obtained using Pt CEs (6.89%). The noticeable photovoltaic performance exhibited by the N-doped composite electrodes was attributed to the low potential value among peak-to-peak separation along with reduced charge transfer resistance at CE/electrolyte interface.

Khan et al. fabricated a $Co_3O_4$@f-MWCNTs@N-RGO based CE for DSSCs and achieved up to 8.42% conversion efficiency which is noticeably higher than that shown by the counterpart platinum based counter electrode (PCE~7.81%). The high catalytic performance due the large current density of $Co_3O_4$@f-MWCNTs@N-RGO CE as compared to all other electrodes[190].

Al-bahrani et al. [191] studied the preparation of a graphene nanosheets/MWCNTs and polyaniline (GNS/MWCNT/PANI) rough and porous nanocomposite via an in-situ polymerization method and successfully applied it a low cost and highly efficient CE for DSSCs using a spin coating procedure (see **Fig. 18**). The combined of the greater intrinsic catalytic performance of PANI and excellent electrical conductivity of GNS/MWCNT led to a reduced charge transfer resistance at the electrolyte/CE interface, along with the consequent

improvement of both the catalytic activity as well as photovoltaic performance of the hybrid composite CE. When incorporated in the DSSC, the GNS/MWCNT/PANI CE showed a noticeable power conversion efficiency of 7.52% greater than that obtained with the Pt CE (6.69%) in similar conditions.

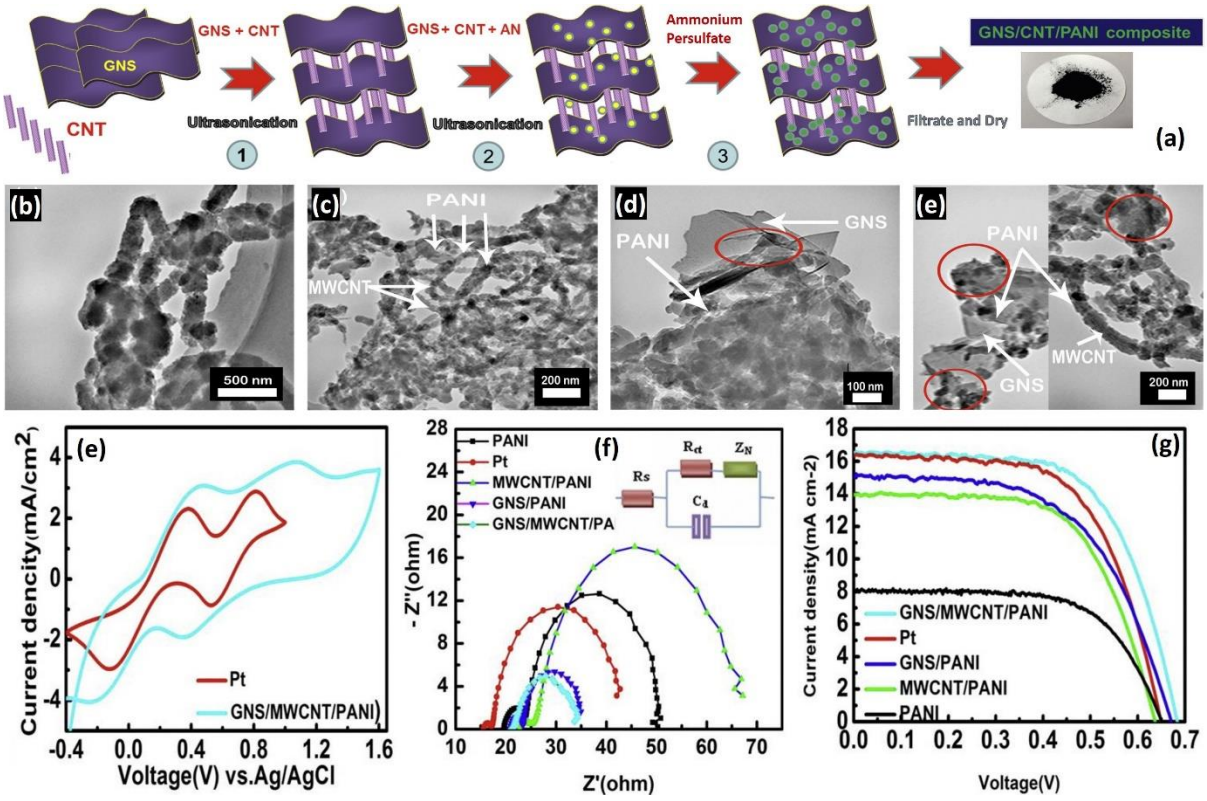


**Fig. 18. Synthesis protocols for graphene nanosheets (GNS)/CNT/PANI composite (a). TEM images of PANI (b), CNT/PANI (c), GNS/PANI (d), and GNS/CNT/PANI (e). CV comparison for Pt and GNS/CNT/PANI electrodes (f). EIS analysis of various CEs and equivalent circuit whereas $R_s$~ series resistance, $R_{ct}$~charge-transfer resistance, $C_d$~ double layer capacitance and $Z_N$~diffusion impedance (g). J-V curves of CEs based on Pt, GNS/CNT/PANI, GNS/PANI, CNT/PANI and PANI (h). (Reproduced with the permission from Ref. [191], Copyright 2014 Elsevier)**

Lin et al. proposed the synthesis through a facile electrophoretic deposition technique of a novel hybrid material by combining molybdenum disulfide and reduced graphene oxide

nanocomposites with carbon nanotubes ($MoS_2$/RGO-CNTs) and its exploitation as a low cost CE [192]. As highlighted by a detailed electrochemical analysis, the incorporation of CNTs conductive grids provided extra pathways for electronic transportation, thus resulting in the increase of the charge transfer rate at the CE/electrolyte interface and in a markedly enhanced electrocatalytic activity in the hybrid electrode compared with that of $MoS_2$/RGO alone. The DSSC assembled with the $MoS_2$/RGO-CNTs CE revealed a highest conversion efficiency of about 7.46%, exceeding that measured with DSSCs based on $MoS_2$/RGO CE (6.82%) and on Pt CE (7.23%). SWCNTs are also incorporated into $MoS_2$.

Yue et al. prepared glucose and PEDOT: PSS assisted SWCNTs-$MoS_2$ composite based CEs using an in-situ hydrothermal method. A promising photo-conversion efficiency of about 8.14%, analogous to that shown by the Pt CE (7.78%), was achieved [193]. These promising results were attributed to the low charge transfer resistance and high catalytic activity. Similarly, carbon nanotube aerogel (CAN) and CoS2 nanoparticle based hybrid CE was prepared by Liu et al. This novel CAN-$CoS_2$ CE showed a high PCE 8.92% than the conventional Pt based CE 7.32% because of the fast ion diffusion and electron transport [194].

Likewise, in another work, the synthesis of a MWCNT and Polyaniline/cobalt sulfide (PANI/MWCNT@$CoS_{1.097}$) nanocomposite was carried out via drop casting technique followed by in situ electropolymerization on FTO glass substrate by means of pulse potentiostatic electropolymerization technique (see **Fig. 19**). The film was then efficiently employed as a metal free CE for DSSCs [195]. The prepared electrode displayed an enhanced electrocatalytic activity compared to PANI and MWCNT@$CoS_{1.097}$ CEs. This can probably be attributed to the high intrinsic electrocatalytic activity of MWCNT@$CoS_{1.097}$ and to its increased adhesion to the FTO glass substrate guaranteed by the conducting PANI. Furthermore, the DSSC based on the PANI/MWCNT@$CoS_{1.097}$ CE achieved an enhanced efficiency of 7.02% with great chemical and electrochemical stability, which is close to that of

the DSSC using Pt CE (7.16%) and higher than those of the DSSCs using PANI (6.06%) and MWCNT@$CoS_{1.097}$ CEs (5.54%).

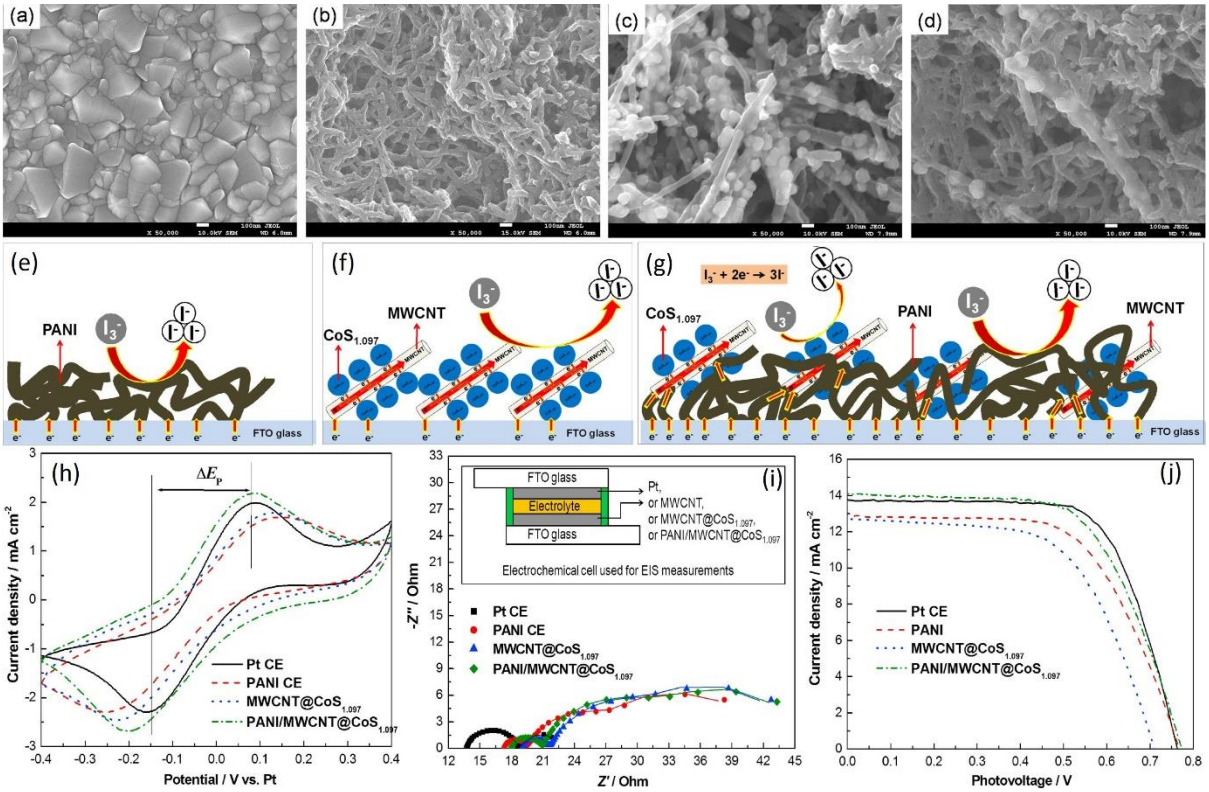


**Fig. 19. SEM images of the FTO substrate (a), PANI (b), MWCNT@$CoS_{1.097}$ (c), and PANI/MWCNT@$CoS_{1.097}$ (d). Schematic illustration for electrocatalytic mechanisms in PANI (e), MWCNT@$CoS_{1.097}$ (f), and PANI/MWCNT@$CoS_{1.097}$ (g). Cyclic voltammetry (h), Nyquist plots (i), and J-V characteristics of DSSCs (j) based on Pt, PANI, MWCNT@$CoS_{1.097}$ and PANI/MWCNT@$CoS_{1.097}$ CEs. (Reproduced with the permission from Ref. [195], Copyright 2014 Elsevier).**

Wang et al. [196] developed a graphitic carbon nitride/MWCNTs composite based CE by refluxing process and polymerization by heating. MWCNTs were very well incorporated and attached to graphitic carbon nitride. The hybrid composite exhibited a superior electrocatalytic performance and a much lower charge diffusion resistance as compared with the individual graphitic carbon nitride and MWCNTs electrodes. The elevated electrocatalytic performance

was possibly due to the synergetic influence of both graphitic carbon nitride and MWCNTs, which respectively show an excellent intrinsic electrocatalytic activity, retain maximum electrical conductivity, and enhanced specific surface area. The DSSC fabricated employing this composite carbon based CE achieved a conversion efficiency of 6.34%, comparable to Pt CE based cell.

Park et al. [197] fabricated CEs based on MWCNTs/mesoporous carbon nanofibers composites using electrospinning and silica template etching and were able to obtain a noticeable overall conversion efficiency of 6.35%. The electrodes showed excellent mesoporous structure, good electrical conductivity, and excellent distribution of CNTs. The most relevant reasons which account for the valuable photovoltaic performance of this mesoporous hybrid carbon based electrode are the relatively reduced charge transport resistance, the large contact area among electrolyte and CE, and the fast electron and ion transfer. The device efficiency was influenced also by the CE thickness, which affects the ionic transfer because it is strictly related to the loading amount of carbon nanofibers. In particular, the DSSCs photovoltaic performance improved while increasing the thickness of the counter electrode.

Wu et. al. [198] prepared a PANI-MWCNTs based CE doped with different cations by coating MWCNTs via an airbrush spraying technique followed by electropolymerziation of aniline monomer containing different cations (see **Fig. 20**). The presence of $Ni^{2+}$ and $Co^{2+}$ ions improved the catalytic activity, while $Cu^{2+}$ showed the opposite effect and $Mn^{2+}$ showed no effect. The highest DSSC efficiency of 6.00% was achieved with $Ni^{2+}$-doped MWCNTs-PANI CE. These distinct behaviors can be probably attributed to the different doping procedures used for metal ions, which are strongly influenced by the empty d-orbital of the metal. $Ni^{2+}$ and $Co^{2+}$ can form a typical octahedral structure with ammonium cationic ligands favorable for electron transport. Conversely, $Mn^{2+}$ exhibits a tetrahedral structure with ammonium cationic ligands and $Cu^{2+}$ establishes a planar structure with the ligands, which retards the electron transport.

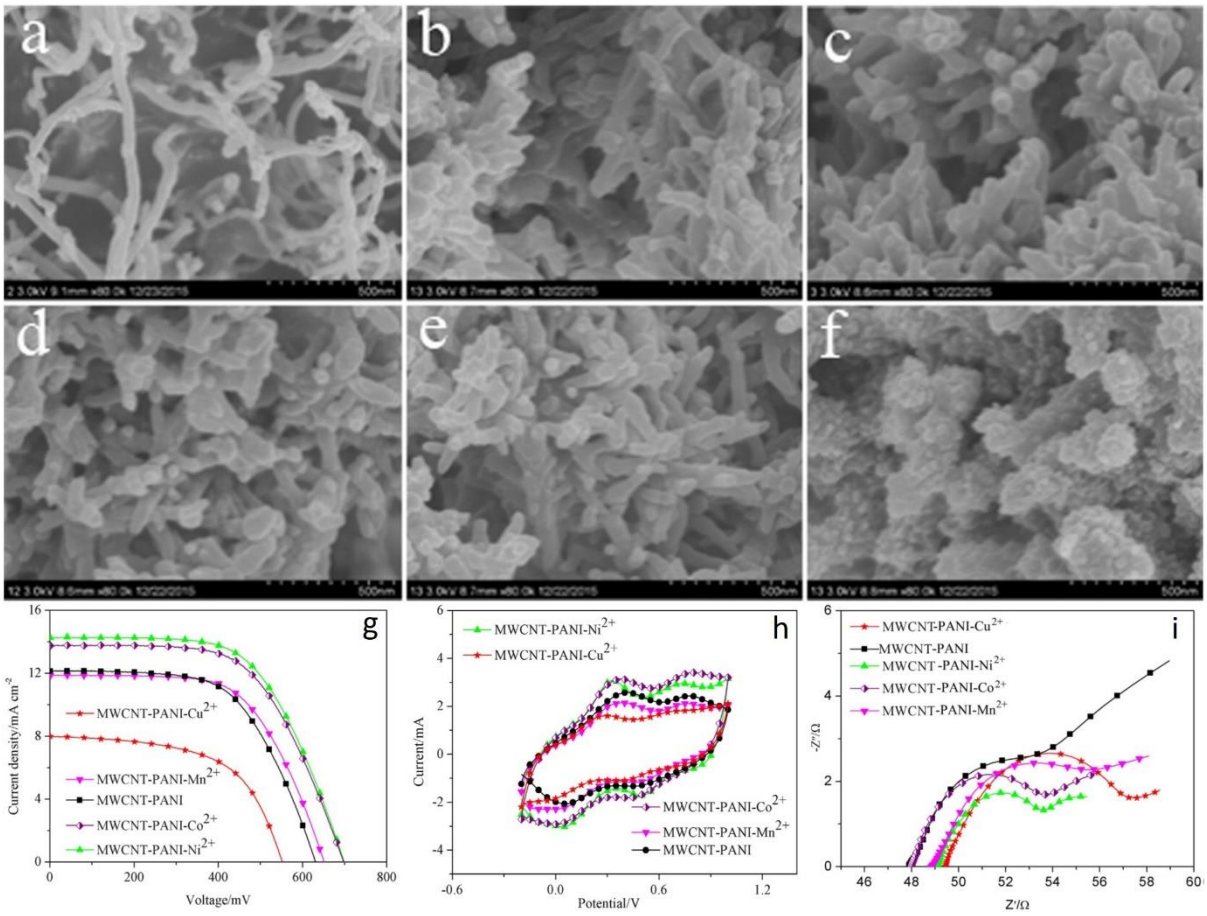


**Fig. 20. SEM images of MWCNT (a), MWCNT-PANI (b), MWCNT-PANI-$Ni^{2+}$ (c), MWCNT-PANI-$Co^{2+}$ (d), MWCNT-PANI-$Mn^{2+}$ (e), and MWCNT-PANI-$Cu^{2+}$ (f). J-V characteristic curves of DSSCs (g), CV of symmetrical cells (h), and Nyquist plots (i) with MWCNT-PANI, MWCNT-PANI-$Cu^{2+}$, MWCNT-PANI-$Ni^{2+}$, MWCNT-PANI-$Mn^{2+}$ and MWCNT-PANI-$Co^{2+}$ CEs. (Reproduced with the permission from Ref [198], Copyright 2016 Elsevier)**

In a very interesting work, Lee et al. synthesized MWCNTs and SWCNTs based CEs for DSSCs starting from a powder of CNTs mixed with $PtCl_4$ solution and an electrolyte [199]. To increase the total conversion efficiency, CNTs were incorporated into the treated $PtCl_4$ electrode and into the electrolyte. The highest efficiency value of 4.36% was attained with the MWCNTs electrode. The SWCNTs and MWCNTs based films were prepared through arc discharge and chemical vapor deposition methods, respectively.

**Tab. 5. Main characteristics and photovoltaic performance of DSSCs fabricated with hybrid CEs**

| No. | CE Material | Deposition method | Photoanode | Sensitizer | Redox couple | PCE (%) | PCE vs Pt (%) | Ref. |
|---|---|---|---|---|---|---|---|---|
| 1 | PANI<br>MWCNTs-$CoS_{1.097}$<br>PANI-MWCNTs-$CoS_{1.097}$ | Drop casting &electropolymerization | $TiO_2$ | N719 | $I_3^-/I^-$ | 6.06<br>5.54<br>7.02 | 7.16 | [195] |
| 2 | MWCNT-PANI<br>MWCNT-PANI-$Ni^{2+}$<br>MWCNT-PANI-$Co^{2+}$<br>MWCNT-PANI-$Mn^{2+}$<br>MWCNT-PANI-$Cu^{2+}$ | Coating over FTO with air brush followed by electropolymerization | $TiO_2$ | N719 | $I_3^-/I^-$ | 4.58<br>6.00<br>5.75<br>4.77<br>2.57 | n.a. | [198] |
| 3 | Organic NMWCNT | Doctor blading | $TiO_2$ | N719 | $I_3^-/I^-$ | 9.55 | 9.89 | [184] |
| 4 | $Co_3O_4$@f-MWCNTs@N-RGO | Doctor blading | $TiO_2$ | N719 | $I_3^-/I^-$ | 8.42 | 7.81 | [190] |
| 5 | GNS/MWCNT/PANI | Spin coating | $TiO_2$ | N719 | $I_3^-/I^-$ | 7.52 | 6.69 | [191] |
| 6 | CAN-$CoS_2$<br>CNA | Hydrothermal & direct pasting | $TiO_2$ | N719 | $I_3^-/I^-$ | 8.92<br>8.28 | 7.32 | [194] |
| 7 | (G-P-A)MWCNTs-$MoS_2$ | Doctor blading | $TiO_2$ | N719 | $I_3^-/I^-$ | 8.14 | 7.78 | [193] |

# 5 Concluding remarks

In recent decades, CNT-based nanomaterials have attracted broad interests at the energy community due to their promising advantages of high conductivity, superior chemical stability, low cost, excellent catalytic activity, mechanical flexibility, and long-term stability. These high performances made them good candidates in DSSC technology to be used as CE materials in substitution of the expensive conventional Pt electrode. In this perspective, this review systematically summarized the recent significant progress in preparing various forms of CNTs-based CEs for DSSCs, and the pivotal factors in determining photovoltaic performance of the above-mentioned electrodes were highlighted in detail. Interestingly, in most cases, the photovoltaic performance of CNTs-based CEs revealed to be comparable to that of Pt electrodes, or even better. Nevertheless, in view of the definitive commercialization of the DSSCs, an intense research effort has yet to be performed to find new effective strategies to further enhance the solar cell photo-conversion efficiency and long-term stability and at the same time to reduce its costs.

**References**


[1] Zervos A. RENEWABLES 2018 -GLOBAL STATUS REPORT. 2018.

[2] Kay Andreas GM. Low cost photovoltaic modules based on dye sensitized nanocrystalline titanium dioxide and carbon powder. Solar Energy Materials and Solar Cells. 1996;44:99-117.

[3] Bolhan A, Ludin NA. Incorporation of Graphene into Counter Electrode to Enhance the Performance of Dye-Sensitized Solar Cells. Malaysian Journal of Analytical Science. 2017;21:1120 - 6.

[4] Badawy WA. A review on solar cells from Si-single crystals to porous materials and quantum dots. Journal of Advanced Research. 2015;6:123-32.

[5] Yang D, Hartman MR, Derrien TL, Hamada S, An D, Yancey KG, et al. DNA Materials: Bridging Nanotechnology and Biotechnology. Accounts of Chemical Research. 2014;47:1902-11.

[6] Qi W, Shapter JG, Wu Q, Yin T, Gao G, Cui D. Nanostructured anode materials for lithium-ion batteries: principle, recent progress and future perspectives. Journal of Materials Chemistry A. 2017;5:19521-40.

[7] Chen S, Zhang Q, Hou Y, Zhang J, Liang X-J. Nanomaterials in medicine and pharmaceuticals: nanoscale materials developed with less toxicity and more efficacy. European Journal of Nanomedicine. 2013;5.

[8] Chaudhary LS, Ghatmale PR, Chavan SS. Review On: Application of Nanotechnology in Computer Science. International Journal of Science and Research (IJSR) 2016;5:1542 - 5.

[9] Sawin JL, Seyboth K, Sverrisson F. RENEWABLES 2017 - GLOBAL STATUS REPORT. In: Sawin JL, editor. Rebewable Energy Policy Network-21. Paris: REN21 Secretariat, Paris, France; 2017.

[10] Zervos A. Renewables 2019, Global Status Report- REN21. 2019.

[11] Togonal AS, Foldyna M, Chen W, Wang JX, Neplokh V, Tchernycheva M, et al. Core–Shell Heterojunction Solar Cells Based on Disordered Silicon Nanowire Arrays. The Journal of Physical Chemistry C. 2016;120:2962-72.

[12] Khadka DB, Kim S, Kim J. Effects of Ge Alloying on Device Characteristics of Kesterite-Based CZTSSe Thin Film Solar Cells. The Journal of Physical Chemistry C. 2016;120:4251-8.

[13] Best Research Cell Efficiences. Golden, Colorado (CO) National Renewable Energy Labortary, US Department of ENERGY, USA; 2020.

[14] Kyaw AKK, Tantang H, Wu T, Ke L, Wei J, Demir HV, et al. Dye-sensitized solar cell with a pair of carbon-based electrodes. Journal of Physics D: Applied Physics. 2012;45:165103.

[15] Kakiage K, Aoyama Y, Yano T, Oya K, Fujisawa J-i, Hanaya M. Highly-efficient dye-sensitized solar cells with collaborative sensitization by silyl-anchor and carboxy-anchor dyes. Chemical communications. 2015;51:15894-7.

[16] Ahmed U, Alizadeh M, Rahim NA, Shahabuddin S, Ahmed MS, Pandey AK. A comprehensive review on counter electrodes for dye sensitized solar cells: A special focus on Pt-TCO free counter electrodes. Solar Energy. 2018;174:1097-125.

[17] Choi J, Song S, Horantner MT, Snaith HJ, Park T. Well-Defined Nanostructured, Single-Crystalline TiO2 Electron Transport Layer for Efficient Planar Perovskite Solar Cells. ACS nano. 2016;10:6029-36.

[18] Pazos-Outón LM, Xiao TP, Yablonovitch E. Fundamental Efficiency Limit of Lead Iodide Perovskite Solar Cells. The journal of physical chemistry letters. 2018;9:1703-11.

[19] Jayawardena KD, Rozanski LJ, Mills CA, Beliatis MJ, Nismy NA, Silva SR. 'Inorganics-in-organics': recent developments and outlook for 4G polymer solar cells. Nanoscale. 2013;5:8411-27.

[20] Azpiroz JM, Infante I, De Angelis F. First-Principles Modeling of Core/Shell Quantum Dot Sensitized Solar Cells. The Journal of Physical Chemistry C. 2015;119:12739-48.

[21] Sanehira EM, Marshall AR, Christians JA, Harvey SP, Ciesielski PN, Wheeler LM, et al. Enhanced mobility CsPbI3 quantum dot arrays for record-efficiency, high-voltage photovoltaic cells. Sci Adv. 2017;3:eaao4204.

[22] Jin J, Zhang X, He T. Self-Assembled CoS2 Nanocrystal Film as an Efficient Counter Electrode for Dye-Sensitized Solar Cells. The Journal of Physical Chemistry C. 2014;118:24877-83.

[23] O'Regan BG, Michael. A low-cost, high-efficiency solar cell based on dye-sensitized colloidal TiO2 films. Nature. 1991;353:737-40.

[24] Chen Y, Zhang H, Chen Y, Lin J. Study on Carbon Nanocomposite Counterelectrode for Dye-Sensitized Solar Cells. Journal of Nanomaterials. 2012;2012:1-6.

[25] Xue Y, Liu J, Chen H, Wang R, Li D, Qu J, et al. Nitrogen-doped graphene foams as metal-free counter electrodes in high-performance dye-sensitized solar cells. Angewandte Chemie. 2012;51:12124-7.

[26] Kroto HWH, J. R. O'Brien, S. C. Curl, R. F. Smalley, R. E. C60 Buckminster fullerene. Nature. 1985;318:162-3.

[27] Sumio I. Helical Microtubules of graphitic carbon. Nature. 1991;354:56-8.

[28] Geim AK, Novoselov KS. The rise of graphene. Nat Mater. 2007;6:183-91.

[29] Koprinarov N, Stefanov R, Pchelarov G, Konstantinova M, Stambolova I. Carbon electrodes for solar cells and other semiconductor devices. Synthetic Metals. 1996;77:47-9.

[30] sedghi Am, nourmohammadi hoda. Effect of Multi Walled Carbon Nanotubes as Counter Electrode on Dye Sensitized Solar Cells. International Journal of ELECTROCHEMICAL SCIENCE. 2014;9:2029-37.

[31] Jha N, Ramesh P, Bekyarova E, Tian X, Wang F, Itkis ME, et al. Functionalized single-walled carbon nanotube-based fuel cell benchmarked against US DOE 2017 technical targets. Scientific reports. 2013;3:2257.

[32] Dai L, Chang DW, Baek JB, Lu W. Carbon nanomaterials for advanced energy conversion and storage. Small. 2012;8:1130-66.

[33] Landi BJ, Ganter MJ, Cress CD, DiLeo RA, Raffaelle RP. Carbon nanotubes for lithium ion batteries. Energy & Environmental Science. 2009;2:638-54.

[34] Rangom Y, Tang XS, Nazar LF. Carbon Nanotube-Based Supercapacitors with Excellent ac Line Filtering and Rate Capability via Improved Interfacial Impedance. ACS nano. 2015;9:7248-55.

[35] Hwang S, Batmunkh M, Nine MJ, Chung H, Jeong H. Dye-sensitized solar cell counter electrodes based on carbon nanotubes. Chemphyschem : a European journal of chemical physics and physical chemistry. 2015;16:53-65.

[36] Ahmad MS, Pandey AK, Rahim NA, Shahabuddin S, Tyagi SK. Chemical sintering of TiO2 based photoanode for efficient dye sensitized solar cells using Zn nanoparticles. Ceramics International. 2018;44:18444-9.

[37] Saltan GM, Dinçalp H, Kıran M, Zafer C, Erbaş SÇ. Novel organic dyes based on phenyl-substituted benzimidazole for dye sensitized solar cells. Materials Chemistry and Physics. 2015;163:387-93.

[38] Gong J, Liang J, Sumathy K. Review on dye-sensitized solar cells (DSSCs): Fundamental concepts and novel materials. Renewable and Sustainable Energy Reviews. 2012;16:5848-60.

[39] Andualem A, Demiss S. Review on Dye-Sensitized Solar Cells (DSSCs). Edelweiss Applied Science and Technology. 2018;2:6.

[40] Polo AS, Itokazu MK, Murakami Iha NY. Metal complex sensitizers in dye-sensitized solar cells. Coordination Chemistry Reviews. 2004;248:1343-61.

[41] Zhang Y, Ren P, Li Y, Su R, Zhao M. Optical Absorption and Electron Injection of 4-(Cyanomethyl)benzoic Acid Based Dyes: A DFT Study. Journal of Chemistry. 2015;2015:1-9.

[42] Calogero G, Di Marco G, Cazzanti S, Caramori S, Argazzi R, Di Carlo A, et al. Efficient dye-sensitized solar cells using red turnip and purple wild sicilian prickly pear fruits. International journal of molecular sciences. 2010;11:254-67.

[43] Qin Y, Peng Q. Ruthenium Sensitizers and Their Applications in Dye-Sensitized Solar Cells. International Journal of Photoenergy. 2012;2012:1-21.

[44] Suriati SMS, Mukhzeer Alahmed Z.A , Chyský,J Reshak,A. H Materials for Enhanced Dye-sensitized Solar Cell Performance Electrochemical Application. International Journal of ELECTROCHEMICAL SCIENCE. 2015;10:2859 - 71.

[45] Moehl T, Im JH, Lee YH, Domanski K, Giordano F, Zakeeruddin SM, et al. Strong Photocurrent Amplification in Perovskite Solar Cells with a Porous TiO2 Blocking Layer under Reverse Bias. The journal of physical chemistry letters. 2014;5:3931-6.

[46] Yu Q, Wang Y, Yi Z, Zu N, Zhang J, Zhang M, et al. High-efficiency dye-sensitized solar cells: the influence of lithium ions on exciton dissociation, charge recombination, and surface states. ACS nano. 2010;4:6032-8.

[47] Wei L, Na Y, Yang Y, Fan R, Wang P, Li L. Efficiency of ruthenium dye sensitized solar cells enhanced by 2,6-bis[1-(phenylimino)ethyl]pyridine as a co-sensitizer containing methyl substituents on its phenyl rings. Physical chemistry chemical physics : PCCP. 2015;17:1273-80.

[48] Lee C-P, Lin RY-Y, Lin L-Y, Li C-T, Chu T-C, Sun S-S, et al. Recent progress in organic sensitizers for dye-sensitized solar cells. RSC Advances. 2015;5:23810-25.

[49] Yella A, Lee HW, Tsao HN, Yi C, Chandiran AK, Nazeeruddin MK, et al. Porphyrin-Sensitized Solar Cells with Cobalt (II/III)-Based Redox Electrolyte Exceed 12 Percent Efficiency. Science. 2011;334:629-34.

[50] Mathew S, Yella A, Gao P, Humphry-Baker R, Curchod BF, Ashari-Astani N, et al. Dye-sensitized solar cells with 13% efficiency achieved through the molecular engineering of porphyrin sensitizers. Nature chemistry. 2014;6:242-7.

[51] Kenji Kakiage aYA, a Toru Yano,*a Keiji Oya,a Jun-ichi Fujisawab and Minoru Hanaya*. Highly-efficient dye-sensitized solar cells with collaborative sensitization by silyl-anchor and carboxy-anchor dyes†. J Name. 2013.

[52] Nagarajan B, Kushwaha S, Elumalai R, Mandal S, Ramanujam K, Raghavachari D. Novel ethynyl-pyrene substituted phenothiazine based metal free organic dyes in DSSC with 12% conversion efficiency. Journal of Materials Chemistry A. 2017;5:10289-300.

[53] Wang J, Wu H, Jin L, Zhang J, Yuan Y, Wang P. A Perylene-Based Polycyclic Aromatic Hydrocarbon Electron Donor for a Highly Efficient Solar Cell Dye. ChemSusChem. 2017;10:2962-7.

[54] Jamalullail N, Mohamad IS, Norizan MN, Baharum NA. Short Review: Natural Pigments Photosensitizer for Dye-Sensitized Solar Cell (DSSC). 15th Student Conference on Research and Development (SCOReD). Perlis, Malaysia.: IEEE; 2017.

[55] Hyo JLK, Dae-Young Yoo, JungSuk Bang, Jiwon Kim,Sungjee Park,Su Moon Anchoring Cadmium Chalcogenide Quantum Dots (QDs) onto Stable Oxide Semiconductors for QD Sensitized Solar Cells. Bulletin Korean Chemical Society. 2007;28 953-8.

[56] Pan Z, Rao H, Mora-Seró I, Bisquert J, Zhong X. Quantum dot-sensitized solar cells. Chemical Society reviews. 2018;47:7659-702.

[57] Kojima A, Teshima K, Shirai Y, Miyasaka T. Organometal halide perovskites as visible-light sensitizers for photovoltaic cells. Journal of the American Chemical Society. 2009;131:6050-1.

[58] Shi Z, Jayatissa A. Perovskites-Based Solar Cells: A Review of Recent Progress, Materials and Processing Methods. Materials. 2018;11.

[59] Liu X, Fang J, Liu Y, Lin T. Progress in nanostructured photoanodes for dye-sensitized solar cells. Frontiers of Materials Science. 2016;10:225-37.

[60] Fan K, Yu J, Ho W. Improving photoanodes to obtain highly efficient dye-sensitized solar cells: a brief review. Materials Horizons. 2017;4:319-44.

[61] Cao Y, Dong Y-J, Feng H-L, Chen H-Y, Kuang D-B. Electrospun TiO 2 nanofiber based hierarchical photoanode for efficient dye-sensitized solar cells. Electrochimica Acta. 2016;189:259-64.

[62] Lai FI, Yang JF, Kuo SY. Efficiency Enhancement of Dye-Sensitized Solar Cells' Performance with ZnO Nanorods Grown by Low-Temperature Hydrothermal Reaction. Materials (Basel). 2015;8:8860-7.

[63] Mehmood U, Rahman S-u, Harrabi K, Hussein IA, Reddy BVS. Recent Advances in Dye Sensitized Solar Cells. Advances in Materials Science and Engineering. 2014;2014:1-12.

[64] Cho T-Y, Ko K-W, Yoon S-G, Sekhon SS, Kang MG, Hong Y-S, et al. Efficiency enhancement of flexible dye-sensitized solar cell with sol–gel formed Nb2O5 blocking layer. Current Applied Physics. 2013;13:1391-6.

[65] Lin HCS, Chaochin Li, Wen Ren The effect of ZnO coatings on the performance of WO3 dye-sensit. 2013:1063-9.

[66] Jiang Q, Gao J, Yi L, Hu G, Zhang J. Enhanced performance of dye-sensitized solar cells based on P25/Ta2O5 composite films. Applied Physics A. 2016;122:442-8.

[67] Lee H, Wang M, Chen P, Gamelin DR, Zakeeruddin SM, Gratzel M, et al. Efficient CdSe quantum dot-sensitized solar cells prepared by an improved successive ionic layer adsorption and reaction process. Nano letters. 2009;9:4221-7.

[68] Kim SF, Brent Eisler,Hans Jurgen Bawendi, Moungi Type-II Quantum Dots: CdTe/CdSe(Core/Shell) and CdSe/ZnTe(Core/Shell) Heterostructures. journal of american chemical society. 2003;125:11466-7.

[69] Lee HJ, Lee Y, Altantuya U. Quantum Dot (QD) Sensitizer on the Surface of TiO2Film: Effect of Metal Salt Anions Dissolved in Chemical Bath on the Distribution Density of SILAR-Grown PbS QDs. Journal of the Korean Chemical Society. 2015;59:97-102.

[70] Brown MD, Suteewong T, Kumar RS, D'Innocenzo V, Petrozza A, Lee MM, et al. Plasmonic dye-sensitized solar cells using core-shell metal-insulator nanoparticles. Nano letters. 2011;11:438-45.

[71] Costenaro D, Bisio C, Carniato F, Gatti G, Oswald F, Meyer TB, et al. Size effect of synthetic saponite-clay in quasi-solid electrolyte for dye-sensititized solar cells. Solar Energy Materials and Solar Cells. 2013;117:9-14.

[72] Hassan HC, Abidin ZHZ, Chowdhury FI, Arof AK. A High Efficiency Chlorophyll Sensitized Solar Cell with Quasi Solid PVA Based Electrolyte. International Journal of Photoenergy. 2016;2016:1-9.

[73] Wu J, Lan Z, Hao S, Li P, Lin J, Huang M, et al. Progress on the electrolytes for dye-sensitized solar cells. Pure and Applied Chemistry. 2008;80:2241-58.

[74] Wu J, Lan Z, Lin J, Huang M, Huang Y, Fan L, et al. Electrolytes in dye-sensitized solar cells. Chemical reviews. 2015;115:2136-73.

[75] Yang Y, Tao J, Ma L. Study on Properties of Quasi Solid Polymer Electrolyte Based on PVdF-PMMA Blend for Dye-Sensitized Solar Cells. Materials Science Forum. 2009;610-613:347-52.

[76] Wu J, Li Y, Tang Q, Yue G, Lin J, Huang M, et al. Bifacial dye-sensitized solar cells: A strategy to enhance overall efficiency based on transparent polyaniline electrode. Scientific reports. 2014;4:4028.

[77] Tang Z, Wu J, Zheng M, Huo J, Lan Z. A microporous platinum counter electrode used in dye-sensitized solar cells. Nano Energy. 2013;2:622-7.

[78] Chen X, Tang Q, He B, Lin L, Yu L. Platinum-Free Binary Co-Ni Alloy Counter Electrodes for Efficient Dye-Sensitized Solar Cells. Angewandte Chemie International Edition. 2014;53:10799-803.

[79] Lin X, Wu M, Wang Y, Hagfeldt A, Ma T. Novel counter electrode catalysts of niobium oxides supersede Pt for dye-sensitized solar cells. Chemical communications. 2011;47:11489-91.

[80] Ozel F, Sarilmaz A, Istanbullu B, Aljabour A, Kus M, Sonmezoglu S. Penternary chalcogenides nanocrystals as catalytic materials for efficient counter electrodes in dye-synthesized solar cells. Scientific reports. 2016;6:29207.

[81] Li GR, Song J, Pan GL, Gao XP. Highly Pt-like electrocatalytic activity of transition metal nitrides for dye-sensitized solar cells. Energy & Environmental Science. 2011;4:1680-3.

[82] Zhao W, Zhu X, Bi H, Cui H, Sun S, Huang F. Novel two-step synthesis of NiS nanoplatelet arrays as efficient counter electrodes for dye-sensitized solar cells. Journal of Power Sources. 2013;242:28-32.

[83] Wu M, Lin X, Wang Y, Wang L, Guo W, Qi D, et al. Economical Pt-free catalysts for counter electrodes of dye-sensitized solar cells. Journal of the American Chemical Society. 2012;134:3419-28.

[84] Dou YY, Li GR, Song J, Gao XP. Nickel phosphide-embedded graphene as counter electrode for dye-sensitized solar cells. Physical chemistry chemical physics : PCCP. 2012;14:1339-42.

[85] Al Mamun MZ, Haimin Porun ,Liu Yun Wang, Jun Caoa Zhao, Huijun. Directly hydrothermal growth of ultrathin MoS2 nanostructured films as high performance counter electrodes for dye sensitised solar cells. RSC Advance. 2014;4:21277-83.

[86] Zhou Q, Shi G. Conducting Polymer-Based Catalysts. Journal of the American Chemical Society. 2016;138:2868-76.

[87] Veerappan G, Bojan K, Rhee SW. Sub-micrometer-sized graphite as a conducting and catalytic counter electrode for dye-sensitized solar cells. ACS applied materials & interfaces. 2011;3:857-62.

[88] Yen M-Y, Teng C-C, Hsiao M-C, Liu P-I, Chuang W-P, Ma C-CM, et al. Platinum nanoparticles/graphene composite catalyst as a novel composite counter electrode for high performance dye-sensitized solar cells. Journal of Materials Chemistry. 2011;21:12880.

[89] Widodo S, Wiranto G, Hidayat MN. Fabrication of Dye Sensitized Solar Cells with Spray Coated Carbon Nano Tube (CNT) Based Counter Electrodes. Energy Procedia. 2015;68:37-44.

[90] Trancik JE, Barton SC, Hone J. Transparent and catalytic carbon nanotube films. Nano letters. 2008;8:982-7.

[91] Huang Z, Liu X, Li K, Li D, Luo Y, Li H, et al. Application of carbon materials as counter electrodes of dye-sensitized solar cells. Electrochemistry Communications. 2007;9:596-8.

[92] Cheng Y, Liu J. Carbon Nanomaterials for Flexible Energy Storage. Materials Research Letters. 2013;1:175-92.

[93] Nabae Y, Nagata S, Hayakawa T, Niwa H, Harada Y, Oshima M, et al. Pt-free carbon-based fuel cell catalyst prepared from spherical polyimide for enhanced oxygen diffusion. Scientific reports. 2016;6:23276.

[94] Rasu Ramachandran2 VM, Shen-Ming Chen1,*, George peter Gnana kumar3, Pandi Gajendran2, Natarajan Biruntha Devi4, Rajkumar Devasenathipathy1. Recent Progress in Electrode Fabrication Materials and Various Insights in Solar cells: Review. international Journal of ELECTROCHEMICAL SCIENCE. 2015;10:3301-18.

[95] Candelaria SL, Shao Y, Zhou W, Li X, Xiao J, Zhang J-G, et al. Nanostructured carbon for energy storage and conversion. Nano Energy. 2012;1:195-220.

[96] Chen T, Dai L. Carbon nanomaterials for high-performance supercapacitors. Materials Today. 2013;16:272-80.

[97] Guofa Dong‡ a, b, Ming Fang‡,a,b, Hongtao Wangc, Senpo Yipa,b, Ho-Yuen Cheungd, Fengyun Wange, Chun- Yuen Wongd, Saitak Chu*,a and Johnny C. Ho*. Insight into the Electrochemical Activation of Carbon-Based Cathodes for Hydrogen Evolution Reaction. Journal of Materials Chemistry. 2015:1-9.

[98] López-Naranjo EJ, González-Ortiz LJ, Apátiga LM, Rivera-Muñoz EM, Manzano-Ramírez A. Transparent Electrodes: A Review of the Use of Carbon-Based Nanomaterials. Journal of Nanomaterials. 2016;2016:1-12.

[99] Liu X, Dai L. Carbon-based metal-free catalysts. Nature Reviews Materials. 2016;1:16064.

[100] Xu Y, Kraft M, Xu R. Metal-free carbonaceous electrocatalysts and photocatalysts for water splitting. Chemical Society reviews. 2016;45:3039-52.

[101] Gundiah G, Govindaraj A, Rajalakshmi N, Dhathathreyan KS, Rao CNR. Hydrogen storage in carbon nanotubes and related materials. Journal of Materials Chemistry. 2003;13:209-13.

[102] Gupta VIaA. Carbon Nanotubes A Successful Hydrogen

Storage Medium. International Journal of Chemical, Molecular, Nuclear, Materials and Metallurgical Engineering. 2013;7:678-81.

[103] Roy-Mayhew JD, Boschloo G, Hagfeldt A, Aksay IA. Functionalized graphene sheets as a versatile replacement for platinum in dye-sensitized solar cells. ACS applied materials & interfaces. 2012;4:2794-800.

[104] Lee WJ, Ramasamy E, Lee DY, Song JS. Efficient dye-sensitized solar cells with catalytic multiwall carbon nanotube counter electrodes. ACS applied materials & interfaces. 2009;1:1145-9.

[105] Imoto K, Takahashi K, Yamaguchi T, Komura T, Nakamura J-i, Murata K. High-performance carbon counter electrode for dye-sensitized solar cells. Solar Energy Materials and Solar Cells. 2003;79:459-69.

[106] Murakami TN, Ito S, Wang Q, Nazeeruddin MK, Bessho T, Cesar I, et al. Highly Efficient Dye-Sensitized Solar Cells Based on Carbon Black Counter Electrodes. Journal of The Electrochemical Society. 2006;153:A2255.

[107] Chou C-S, Chen C-Y, Lin S-H, Lu W-H, Wu P. Preparation of TiO2/bamboo-charcoal-powder composite particles and their applications in dye-sensitized solar cells. Advanced Powder Technology. 2015;26:711-7.

[108] Gupta R, Kumar R, Sharma A, Verma N. Novel Cu-carbon nanofiber composites for the counter electrodes of dye-sensitized solar cells. International Journal of Energy Research. ===2015;39:668-80.

[109] Suzuki K, Yamaguchi M, Kumagai M, Yanagida S. Application of Carbon Nanotubes to Counter Electrodes of Dye-sensitized Solar Cells. Chemistry Letters. 2003;32:28-9.

[110] Kouhnavard M, Ludin NA, Ghaffari BV, Sopian K, Ikeda S. Carbonaceous materials and their advances as a counter electrode in dye-sensitized solar cells: challenges and prospects. ChemSusChem. 2015;8:1510-33.

[111] Zhang DW, Li XD, Chen S, Tao F, Sun Z, Yin XJ, et al. Fabrication of double-walled carbon nanotube counter electrodes for dye-sensitized solar sells. Journal of Solid State Electrochemistry. 2009;14:1541-6.

[112] Siuzdak K, Klein M, Sawczak M, Wróblewski G, Słoma M, Jakubowska M, et al. Spray-deposited carbon-nanotube counter-electrodes for dye-sensitized solar cells. physica status solidi (a). 2016;213:1157-64.

[113] Chen J-Z, Wang C, Hsu C-C, Cheng IC. Ultrafast synthesis of carbon-nanotube counter electrodes for dye-sensitized solar cells using an atmospheric-pressure plasma jet. Carbon. 2016;98:34-40.

[114] Ramasamy E, Lee WJ, Lee DY, Song JS. Spray coated multi-wall carbon nanotube counter electrode for tri-iodide (I3-) reduction in dye-sensitized solar cells. Electrochemistry Communications. 2008;10:1087-9.

[115] Ahn JY, Kim JH, Kim JM, Lee D, Kim SH. Multiwalled carbon nanotube thin films prepared by aerosol deposition process for use as highly efficient Pt-free counter electrodes of dye-sensitized solar cells. Solar Energy. 2014;107:660-7.

[116] Dumlich H, Gegg M, Hennrich F, Reich S. Bundle and chirality influences on properties of carbon nanotubes studied with van der Waals density functional theory. physica status solidi (b). 2011;248:2589-92.

[117] Ibrahim I, Zhang Y, Popov A, Dunsch L, Büchner B, Cuniberti G, et al. Growth of all-carbon horizontally aligned single-walled carbon nanotubes nucleated from fullerene-based structures. Nanoscale Research Letters. 2013;8:1-6.

[118] Dong P, Pint CL, Hainey M, Mirri F, Zhan Y, Zhang J, et al. Vertically aligned single-walled carbon nanotubes as low-cost and high electrocatalytic counter electrode for dye-sensitized solar cells. ACS applied materials & interfaces. 2011;3:3157-61.

[119] Nam JG, Park YJ, Kim BS, Lee JS. Enhancement of the efficiency of dye-sensitized solar cell by utilizing carbon nanotube counter electrode. Scripta Materialia. 2010;62:148-50.

[120] Seo SH, Kim SY, Koo BK, Cha SI, Lee DY. Influence of electrolyte composition on the photovoltaic performance and stability of dye-sensitized solar cells with multiwalled carbon nanotube catalysts. Langmuir. 2010;26:10341-6.

[121] Zhang D, Li X, Chen S, Sun Z, Jiang Yin X, Huang S. Performance of dye-sensitized solar cells with various carbon nanotube counter electrodes. Microchimica Acta. 2011;174:73-9.

[122] Younas M, Gondal MA, Dastageer MA, Baig U. Fabrication of cost effective and efficient dye sensitized solar cells with WO3-TiO2 nanocomposites as photoanode and MWCNT as Pt-free counter electrode. Ceramics International. 2019;45:936-47.

[123] Siwach B, Mohan D, Singh KK, Kumar A, Barala M. Effect of carbonaceous counter electrodes on the performance of ZnO-graphene nanocomposites based dye sensitized solar cells. Ceramics International. 2018;44:21120-6.

[124] Arbab AA, Peerzada MH, Sahito IA, Jeong SH. A complete carbon counter electrode for high performance quasi solid state dye sensitized solar cell. Journal of Power Sources. 2017;343:412-23.

[125] Sun KC, Arbab AA, Sahito IA, Qadir MB, Choi BJ, Kwon SC, et al. A PVdF-based electrolyte membrane for a carbon counter electrode in dye-sensitized solar cells. RSC Advances. 2017;7:20908-18.

[126] Chew JW, Khanmirzaei MH, Numan A, Omar FS, Ramesh K, Ramesh S. Performance studies of ZnO and multi walled carbon nanotubes-based counter electrodes with gel polymer electrolyte for dye-sensitized solar cell. Materials Science in Semiconductor Processing. 2018;83:144-9.

[127] Niyogi S, Hamon MA, Hu H, Zhao B, Bhowmik P, Sen R, et al. Chemistry of single-walled carbon nanotubes. Acc Chem Res. 2002;35:1105-13.

[128] Marshall MW, Popa-Nita S, Shapter JG. Measurement of functionalised carbon nanotube carboxylic acid groups using a simple chemical process. Carbon. 2006;44:1137-41.

[129] Chou C-S, Huang C-I, Yang R-Y, Wang C-P. The effect of SWCNT with the functional group deposited on the counter electrode on the dye-sensitized solar cell. Advanced Powder Technology. 2010;21:542-50.

[130] Arbab AA, Sun KC, Sahito IA, Qadir MB, Jeong SH. Fabrication of highly electro catalytic active layer of multi walled carbon nanotube/enzyme for Pt-free dye sensitized solar cells. Applied Surface Science. 2015;349:174-83.

[131] Monreal-Bernal A, Vilatela JJ, Costa RD. CNT fibres as dual counter-electrode/current-collector in highly efficient and stable dye-sensitized solar cells. Carbon. 2019;141:488-96.

[132] Chen T, Qiu L, Cai Z, Gong F, Yang Z, Wang Z, et al. Intertwined Aligned Carbon Nanotube Fiber Based Dye-Sensitized Solar Cells. Nano letters. 2012;12:2568-72.

[133] Pan S, Yang Z, Li H, Qiu L, Sun H, Peng H. Efficient Dye-Sensitized Photovoltaic Wires Based on an Organic Redox Electrolyte. Journal of the American Chemical Society. 2013;135:10622-5.

[134] Wei Z, Tao Q, Yongchao ZH, SHI, Junqing T. Fabrication and characterization of a multi walled carbon nanotube based counter electrode for dye sensitized solar cells. New carbon material. 2015;30:391-6.

[135] Tai Q, Chen B, Guo F, Xu S, Hu H, Sebo B, et al. In situ prepared transparent polyaniline electrode and its application in bifacial dye-sensitized solar cells. ACS nano. 2011;5:3795-9.

[136] Anothumakkool B, Agrawal I, Bhange SN, Soni R, Game O, Ogale SB, et al. Pt- and TCO-Free Flexible Cathode for DSSC from Highly Conducting and Flexible PEDOT Paper Prepared via in Situ Interfacial Polymerization. ACS applied materials & interfaces. 2016;8:553-62.

[137] Park J-G, Akhtar MS, Li ZY, Cho D-S, Lee W, Yang OB. Application of single walled carbon nanotubes as counter electrode for dye sensitized solar cells. Electrochimica Acta. 2012;85:600-4.

[138] Holubowitch NE, Landon J, Lippert CA, Craddock JD, Weisenberger MC, Liu K. Spray-Coated Multiwalled Carbon Nanotube Composite Electrodes for Thermal Energy Scavenging Electrochemical Cells. ACS applied materials & interfaces. 2016;8:22159-67.

[139] He B, Tang Q, Luo J, Li Q, Chen X, Cai H. Rapid charge-transfer in polypyrrole–single wall carbon nanotube complex counter electrodes: Improved photovoltaic performances of dye-sensitized solar cells. Journal of Power Sources. 2014;256:170-7.

[140] Lee K-M, Chiu W-H, Wei H-Y, Hu C-W, Suryanarayanan V, Hsieh W-F, et al. Effects of mesoscopic poly(3,4-ethylenedioxythiophene) films as counter electrodes for dye-sensitized solar cells. Thin Solid Films. 2010;518:1716-21.

[141] Shin H-J, Jeon SS, Im SS. CNT/PEDOT core/shell nanostructures as a counter electrode for dye-sensitized solar cells. Synthetic Metals. 2011;161:1284-8.

[142] Fan B, Mei X, Sun K, Ouyang J. Conducting polymer/carbon nanotube composite as counter electrode of dye-sensitized solar cells. Applied Physics Letters. 2008;93.

[143] Yun D-J, Jeong YJ, Ra H, Kim J-M, An TK, Rhee S-W, et al. Systematic optimization of MWCNT-PEDOT:PSS composite electrodes for organic transistors and dye-sensitized solar cells: Effects of MWCNT diameter and purity. Organic Electronics. 2018;52:7-16.

[144] Ma J, Yang H, Ren W, Yang Y. Functionalization of aligned carbon nanotubes used as counter electrode for dye-sensitized solar cells. Materials Research Express. 2019;6.

[145] Choi HJ, Shin JE, Lee G-W, Park N-G, Kim K, Hong SC. Effect of surface modification of multi-walled carbon nanotubes on the fabrication and performance of carbon nanotube based counter electrodes for dye-sensitized solar cells. Current Applied Physics. 2010;10:S165-S7.

[146] Li H, Xiao Y, Han G, Zhang Y. A transparent honeycomb-like poly(3,4-ethylenedioxythiophene)/multi-wall carbon nanotube counter electrode for bifacial dye-sensitized solar cells. Organic Electronics. 2017;50:161-9.

[147] Ali A, Shah SM, Bozar S, Kazici M, Keskin B, Kaleli M, et al. Metal-free polymer/MWCNT composite fiber as an efficient counter electrode in fiber shape dye-sensitized solar cells. Nanotechnology. 2016;27:384003.

[148] Mao X, Zhang S, Ma Q, Wan L, Niu H, Qin S, et al. Non-covalent construction of non-Pt counter electrodes for high performance dye-sensitized solar cells. Journal of Sol-Gel Science and Technology. 2015;74:240-8.

[149] Hou W, Xiao Y, Han G, Zhou H. Electro-polymerization of polypyrrole/multi-wall carbon nanotube counter electrodes for use in platinum-free dye-sensitized solar cells. Electrochimica Acta. 2016;190:720-8.

[150] Li H, Xiao Y, Han G, Li M. Honeycomb-like polypyrrole/multi-wall carbon nanotube films as an effective counter electrode in bifacial dye-sensitized solar cells. Journal of Materials Science. 2017;52:8421-31.

[151] Kuliček J, Gemeiner P, Omastová M, Mičušík M. Preparation of polypyrrole/multi-walled carbon nanotube hybrids by electropolymerization combined with a coating method for counter electrodes in dye-sensitized solar cells. Chemical Papers. 2018;72:1651-67.

[152] Cogal S, Ela SE, Cogal GC, Micusik M, Omastova M, Oksuz AU. Plasma-enhanced modification of multiwalled carbon nanotube with conducting polymers for dye sensitized solar cells. Polymer Composites. 2018;39:668-74.

[153] Erten-Ela S, Cogal S, Cogal GC, Oksuz AU. Highly conductive polymer materials based multi-walled carbon nanotubes as counter electrodes for dye-sensitized solar cells. Fullerenes, Nanotubes and Carbon Nanostructures. 2016;24:380-4.

[154] Okumura T, Sugiyo T, Inoue T, Ikegami M, Miyasaka T. Nickel Oxide Hybridized Carbon Film as an Efficient Mesoscopic Cathode for Dye-Sensitized Solar Cells. Journal of The Electrochemical Society. 2013;160:H155-H9.

[155] Wu M, Lin X, Hagfeldt A, Ma T. A novel catalyst of WO2 nanorod for the counter electrode of dye-sensitized solar cells. Chemical communications. 2011;47:4535-7.

[156] Sun H, Qin D, Huang S, Guo X, Li D, Luo Y, et al. Dye-sensitized solar cells with NiS counter electrodes electrodeposited by a potential reversal technique. Energy & Environmental Science. 2011;4:2630.

[157] Kung CW, Chen HW, Lin CY, Huang KC, Vittal R, Ho KC. CoS acicular nanorod arrays for the counter electrode of an efficient dye-sensitized solar cell. ACS nano. 2012;6:7016-25.

[158] Wu J, Yue G, Xiao Y, Huang M, Lin J, Fan L, et al. Glucose aided preparation of tungsten sulfide/multi-wall carbon nanotube hybrid and use as counter electrode in dye-sensitized solar cells. ACS applied materials & interfaces. 2012;4:6530-6.

[159] Wu M, Wang Y, Lin X, Yu N, Wang L, Wang L, et al. Economical and effective sulfide catalysts for dye-sensitized solar cells as counter electrodes. Physical chemistry chemical physics : PCCP. 2011;13:19298-301.

[160] Zhang L, Mulmudi HK, Batabyal SK, Lam YM, Mhaisalkar SG. Metal/metal sulfide functionalized single-walled carbon nanotubes: FTO-free counter electrodes for dye sensitized solar cells. Physical chemistry chemical physics : PCCP. 2012;14:9906-11.

[161] Tai S-Y, Liu C-J, Chou S-W, Chien FS-S, Lin J-Y, Lin T-W. Few-layer MoS2 nanosheets coated onto multi-walled carbon nanotubes as a low-cost and highly electrocatalytic counter electrode for dye-sensitized solar cells. Journal of Materials Chemistry. 2012;22:24753-9.

[162] Theerthagiri J, Senthil RA, Arunachalam P, Madhavan J, Buraidah MH, Santhanam A, et al. Synthesis of various carbon incorporated flower-like MoS2 microspheres as counter electrode for dye-sensitized solar cells. Journal of Solid State Electrochemistry. 2016;21:581-90.

[163] Lu M-N, Dai C-S, Tai S-Y, Lin T-W, Lin J-Y. Hierarchical nickel sulfide/carbon nanotube nanocomposite as a catalytic material toward triiodine reduction in dye-sensitized solar cells. Journal of Power Sources. 2014;270:499-505.

[164] Theerthagiri J, Senthil RA, Arunachalam P, Bhabu KA, Selvi A, Madhavan J, et al. Electrochemical deposition of carbon materials incorporated nickel sulfide composite as counter electrode for dye-sensitized solar cells. Ionics. 2016;23:1017-25.

[165] Yue G, Liu X, Mao Y, Zheng H, Zhang W. A promising hybrid counter electrode of vanadium sulfide decorated with carbon nanotubes for efficient dye-sensitized solar cells. Mater Today Energy. 2017;4:58-65.

[166] Tai S-Y, Lu M-N, Ho H-P, Xiao Y, Lin J-Y. Investigation of carbon nanotubes decorated with cobalt sulfides of different phases as nanocomposite catalysts in dye-sensitized solar cells. Electrochimica Acta. 2014;143:216-21.

[167] Memon AA, Patil SA, Sun KC, Mengal N, Arbab AA, Sahito IA, et al. Carbonous metallic framework of multi-walled carbon Nanotubes/Bi2S3 nanorods as heterostructure composite films for efficient quasi-solid state DSSCs. Electrochimica Acta. 2018;283:997-1005.

[168] Zhang Y, Wang D, Wang Q, Zheng W. One-step synthesized CuS and MWCNTs composite as a highly efficient counter electrode for quantum dot sensitized solar cells. Materials & Design. 2018;160:870-5.

[169] Lin J-Y, Liao J-H, Hung T-Y. A composite counter electrode of CoS/MWCNT with high electrocatalytic activity for dye-sensitized solar cells. Electrochemistry Communications. 2011;13:977-80.

[170] Wu K, Zhao J, Xiong Y, Ruan B, Wu M. Synthesis and performance of La2O3@MWCNT composite materials as Pt-free counter electrodes for dye-sensitized solar cells. Ionics. 2018;24:4055-61.

[171] Raissan Al-bahrani M, Liu L, Ahmad W, Tao J, Tu F, Cheng Z, et al. NiO-NF/MWCNT nanocomposite catalyst as a counter electrode for high performance dye-sensitized solar cells. Applied Surface Science. 2015;331:333-8.

[172] Tantang H, Kyaw AK, Zhao Y, Chan-Park MB, Tok AI, Hu Z, et al. Nitrogen-doped carbon nanotube-based bilayer thin film as transparent counter electrode for dye-sensitized solar cells (DSSCs). Chemistry, an Asian journal. 2012;7:541-5.

[173] Zheng X, Deng J, Wang N, Deng D, Zhang WH, Bao X, et al. Podlike N-doped carbon nanotubes encapsulating FeNi alloy nanoparticles: high-performance counter electrode materials for dye-sensitized solar cells. Angewandte Chemie. 2014;53:7023-7.

[174] Shrestha A, Batmunkh M, Shearer CJ, Yin Y, Andersson GG, Shapter JG, et al. Nitrogen-Doped CNx/CNTs Heteroelectrocatalysts for Highly Efficient Dye-Sensitized Solar Cells. Adv Energy Mater. 2017;7.

[175] Chen M, Zhao G, Shao L-L, Yuan Z-Y, Jing Q-S, Huang K-J, et al. Controlled Synthesis of Nickel Encapsulated into Nitrogen-Doped Carbon Nanotubes with Covalent Bonded Interfaces: The Structural and Electronic Modulation Strategy for an Efficient Electrocatalyst in Dye-Sensitized Solar Cells. Chemistry of Materials. 2017;29:9680-94.

[176] Ou J, Gong C, Xiang J, Liu J. Noble metal-free Co@N-doped carbon nanotubes as efficient counter electrode in dye-sensitized solar cells. Solar Energy. 2018;174:225-30.

[177] Lee KS, Lee WJ, Park NG, Kim SO, Park JH. Transferred vertically aligned N-doped carbon nanotube arrays: use in dye-sensitized solar cells as counter electrodes. Chemical communications. 2011;47:4264-6.

[178] Leu Y-A, Yeh M-H, Lin L-Y, Li T-J, Chang L-Y, Shen S-Y, et al. Thermally Stable Boron-Doped Multiwalled Carbon Nanotubes as a Pt-free Counter Electrode for Dye-Sensitized Solar Cells. ACS Sustainable Chemistry & Engineering. 2016;5:537-46.

[179] Yeh M-H, Leu Y-A, Chiang W-H, Li Y-S, Chen G-L, Li T-J, et al. Boron-doped carbon nanotubes as metal-free electrocatalyst for dye-sensitized solar cells: Heteroatom doping level effect on tri-iodide reduction reaction. Journal of Power Sources. 2018;375:29-36.

[180] Arbab AA, Sun KC, Sahito IA, Qadir MB, Choi YS, Jeong SH. A Novel Activated-Charcoal-Doped Multiwalled Carbon Nanotube Hybrid for Quasi-Solid-State Dye-Sensitized Solar Cell Outperforming Pt Electrode. ACS applied materials & interfaces. 2016;8:7471-82.

[181] Han J, Yu B, Noh Y, Suh YJ, Kim MJ, Yoo K, et al. Properties and Microstructure of the Ru-Coated Carbon Nano Tube Counter Electrode for Dye-Sensitized Solar Cells. Journal of Nanoscience and Nanotechnology. 2014;14:6133-6.

[182] Lu S, Jin S, Meng Y, Chen J, Wang W, Yao J, et al. N, S doped hollow core-shell carbon microspheres to enhance catalytic activity in solar cell. Materials Letters. 2019;250:84-7.

[183] Kim SY, Kim Y, Lee KM, Yoon WS, Lee HS, Lee JT, et al. Fully solution-processed transparent conducting oxide-free counter electrodes for dye-sensitized solar cells: spray-coated single-wall carbon nanotube thin films loaded with chemically-reduced platinum nanoparticles. ACS applied materials & interfaces. 2014;6:13430-7.

[184] Arbab AA, Memon AA, Sahito IA, Mengal N, Sun KC, Ali M, et al. An evidence for an organic N-doped multiwall carbon nanotube heterostructure and its superior electrocatalytic properties for promising dye-sensitized solar cells. Journal of Materials Chemistry A. 2018;6:8307-22.

[185] Xing Y, Zheng X, Wu Y, Li M, Zhang WH, Li C. Nitrogen-doped carbon nanotubes with metal nanoparticles as counter electrode materials for dye-sensitized solar cells. Chemical communications. 2015;51:8146-9.

[186] Kim H, Choi H, Hwang S, Kim Y, Jeon M. Fabrication and characterization of carbon-based counter electrodes prepared by electrophoretic deposition for dye-sensitized solar cells. Nanoscale Res Lett. 2012;7:53.

[187] Chang L-H, Hsieh C-K, Hsiao M-C, Chiang J-C, Liu P-I, Ho K-K, et al. A graphene-multi-walled carbon nanotube hybrid supported on fluorinated tin oxide as a counter electrode of dye-sensitized solar cells. Journal of Power Sources. 2013;222:518-25.

[188] Zhang J, Yu M, Li S, Meng Y, Wu X, Liu J. Transparent conducting oxide-free nitrogen-doped graphene/reduced hydroxylated carbon nanotube composite paper as flexible counter electrodes for dye-sensitized solar cells. Journal of Power Sources. 2016;334:44-51.

[189] Ma J, Li C, Yu F, Chen J. "Brick-like" N-doped graphene/carbon nanotube structure forming three-dimensional films as high performance metal-free counter electrodes in dye-sensitized solar cells. Journal of Power Sources. 2015;273:1048-55.

[190] Khan MW, Yao J, Zhang K, Zuo X, Yang Q, Tang H, et al. Engineering N-reduced graphene oxide wrapped Co3O4@f-MWCNT hybrid for enhance performance dye-sensitized solar cells. Journal of Electroanalytical Chemistry. 2019;844:142-54.

[191] Al-bahrani MR, Xu X, Ahmad W, Ren X, Su J, Cheng Z, et al. Highly efficient dye-sensitized solar cell with GNS/MWCNT/PANI as a counter electrode. Materials Research Bulletin. 2014;59:272-7.

[192] Lin J-Y, Su A-L, Chang C-Y, Hung K-C, Lin T-W. Molybdenum Disulfide/Reduced Graphene Oxide-Carbon Nanotube Hybrids as Efficient Catalytic Materials in Dye-Sensitized Solar Cells. ChemElectroChem. 2015;2:720-5.

[193] Yue G, Ma X, Jiang Q, Tan F, Wu J, Chen C, et al. PEDOT:PSS and glucose assisted preparation of molybdenum disulfide/single-wall carbon nanotubes counter electrode and served in dye-sensitized solar cells. Electrochimica Acta. 2014;142:68-75.

[194] Liu T, Mai X, Chen H, Ren J, Liu Z, Li Y, et al. Carbon nanotube aerogel–CoS2 hybrid catalytic counter electrodes for enhanced photovoltaic performance dye-sensitized solar cells. Nanoscale. 2018;10:4194-201.

[195] Xiao Y, Wang W-Y, Chou S-W, Lin T-W, Lin J-Y. In situ electropolymerization of polyaniline/cobalt sulfide decorated carbon nanotube composite catalyst toward triiodide reduction in dye-sensitized solar cells. Journal of Power Sources. 2014;266:448-55.

[196] Wang G, Kuang S, Zhang J, Hou S, Nian S. Graphitic carbon nitride/multiwalled carbon nanotubes composite as Pt-free counter electrode for high-efficiency dye-sensitized solar cells. Electrochimica Acta. 2016;187:243-8.

[197] Park S-H, Jung H-R, Kim B-K, Lee W-J. MWCNT/mesoporous carbon nanofibers composites prepared by electrospinning and silica template as counter electrodes for dye-sensitized solar cells. Journal of Photochemistry and Photobiology A: Chemistry. 2012;246:45-9.

[198] Wu K, Chen L, Duan C, Gao J, Wu M. Effect of ion doping on catalytic activity of MWCNT-polyaniline counter electrodes in dye-sensitized solar cells. Materials & Design. 2016;104:298-302.

[199] Uk Lee S, Seok Choi W, Hong B. A comparative study of dye-sensitized solar cells added carbon nanotubes to electrolyte and counter electrodes. Solar Energy Materials and Solar Cells. 2010;94:680-5.